Transition Metal-Catalyzed Desymmetrizations Based on C—H Activation Processes

Xandro Vidal, Marc Font, Moisés Gulías, and José L. Mascareñas

Centro Singular de Investigación en Química Biolóxica e Materiais Moleculares (CiQUS), Departamento de Química Orgánica, Universidade de Santiago de Compostela, Santiago de Compostela, Spain

1 Introduction

The generation of asymmetry in reactions involving C—H activation processes catalyzed by transition metal complexes is a topic of increasing interest owing to the synthetic potential of C—H functionalization reactions and the pharmaceutical relevance of chiral products. Not surprisingly, many of the examples hitherto described involve the use of palladium catalysts. This transition metal is easily modulated with ligands, very effective for the C—H activation step, and cycles very well among different oxidation states. However, other precious metals such as rhodium and iridium have also been used in several asymmetric reactions based on C—H activations. Less expensive and more sustainable 3d metals have been only sporadically employed in these types of reactions, but very likely they will be more intensively explored in the years to come. There are different strategies for the enantioselective modification of C—H bonds using chiral transition metal catalysts [1, 2]. More standard approaches are based on the generation of chiral centers by enantiotopic metalation of methylene C—H bonds [3] or on kinetic resolutions based on the different C—H activation rates of either enantiomer of a racemic mixture [4]. Alternatively, when the C—H activation reaction results in the loss of one or more symmetry elements in a prochiral precursor with the resulting metal not bound to a chiral carbon, the enantioselectivity is generated in a formal **desymmetrization** process. These latter types of reactions can be classified into three categories depending on the symmetry element that is lost and the type of chirality resulting from the metalation process (Scheme 1): desymmetrization generating point chirality, axial chirality or planar chirality.

This article makes a comprehensive summary of reactions included within these three categories and in which the enantioselectivity-generating step is the C—H activation. Furthermore, we only include reactions in which the C—H activation takes place via concerted metalation deprotonations, oxidative additions, or similar types of processes. We do not discuss C—H abstractions via metal-oxo or metal-carbene/nitrene reagents, or enzymatic enantioselective C—H activations [1].

Handbook of CH-Functionalization, First Edition. Edited by Debabrata Maiti.

DOI: 10.1002/9783527834242.chf0138

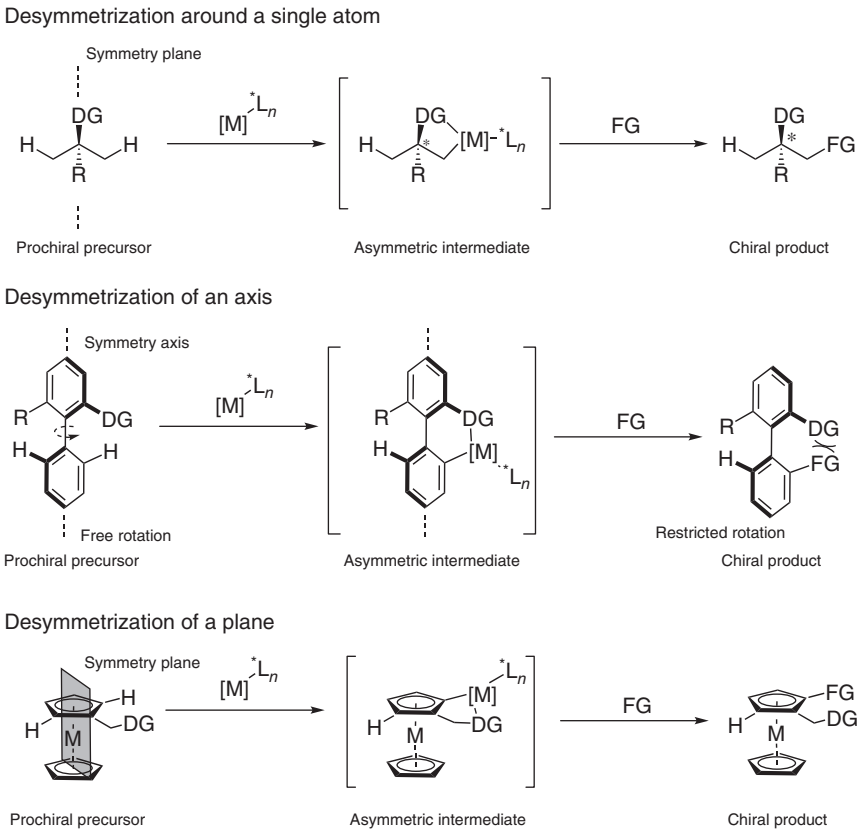

Scheme 1 Different types of desymmetrizations based on metal-promoted C—H activations.

The discussion is organized in three main sections, according to the type of desymmetrization (Scheme 1). Each section is divided considering the mechanism of the C—H activation step and eventually further subdivided, taking into account the hybridization of the reacting carbon. C(sp^2)—H bonds are generally easier to activate than their sp^3-hybridized counterparts; consequently, the number of examples involving enantioselective C(sp^2)—H activations is notably higher [2]. The bonds formed in the reactions are highlighted in bold in the schemes.

2 Desymmetrizations Generating Point Chirality

In this section, we discuss desymmetrization processes leading to the generation of a stereocenter in a carbon atom different to that undergoing the C—H activation. This stereocenter could be formed in an adjacent or distal position to the carbon bound to the transition metal. Reactions entailing the enantioselective C—H activation of enantiotopic protons (methylene functionalization) are not included.

2.1 Reactions Catalyzed by Electrophilic Transition Metal Complexes

We include here enantioselective reactions in which the C—H activation occurs through a concerted metalation–deprotonation (CMD) or similar processe. In these reactions, the metal center is usually confined near the desired reaction site with the aid of a chelating functionality (directing group).

2.1.1 Activation of C(sp^2)—H Bonds

Many of these desymmetrizing reactions have been based on the combination of palladium reagents and monoprotected amino acid (MPAA) ligands. MPAAs facilitate the C—H activation step and are very useful because of their versatility and broad availability [5, 6]. The first studies of desymmetrizations with this kind of ligands were published by the group of Yu in 2008 [7] and consisted of the coupling of prochiral pyridines with alkylboronic acids promoted by a Pd(II) catalyst and an amino acid protected as a menthyl ester (Scheme 2).

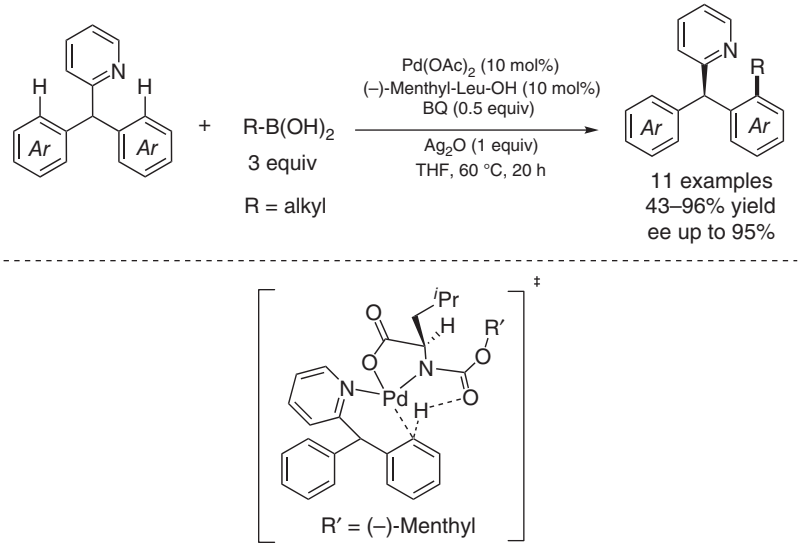

Scheme 2 Pd(II)-catalyzed desymmetrizing alkylation of prochiral pyridines and its proposed transition state. Source: Yu and coworkers.

Another desymmetrization of aromatic C—H bonds, also based on Pd(II)/Pd(0) catalytic redox cycles and MPAA ligands, consisted of a Heck-type coupling of carboxylic acid precursors with electron-deficient alkenes and styrenes and was reported by Yu and coworkers in 2010 (Scheme 3a) [8]. The use of Boc-protected isoleucine as Pd ligand was key to obtain good yields and enantioselectivities. A related olefination process was developed by the group of Wang for the desymmetrization of diaryl sulfoxides, using acetyl-protected leucine as ligand [11]. Yields were generally moderate, but enantioselectivities were higher than 90% ee (Scheme 3b).

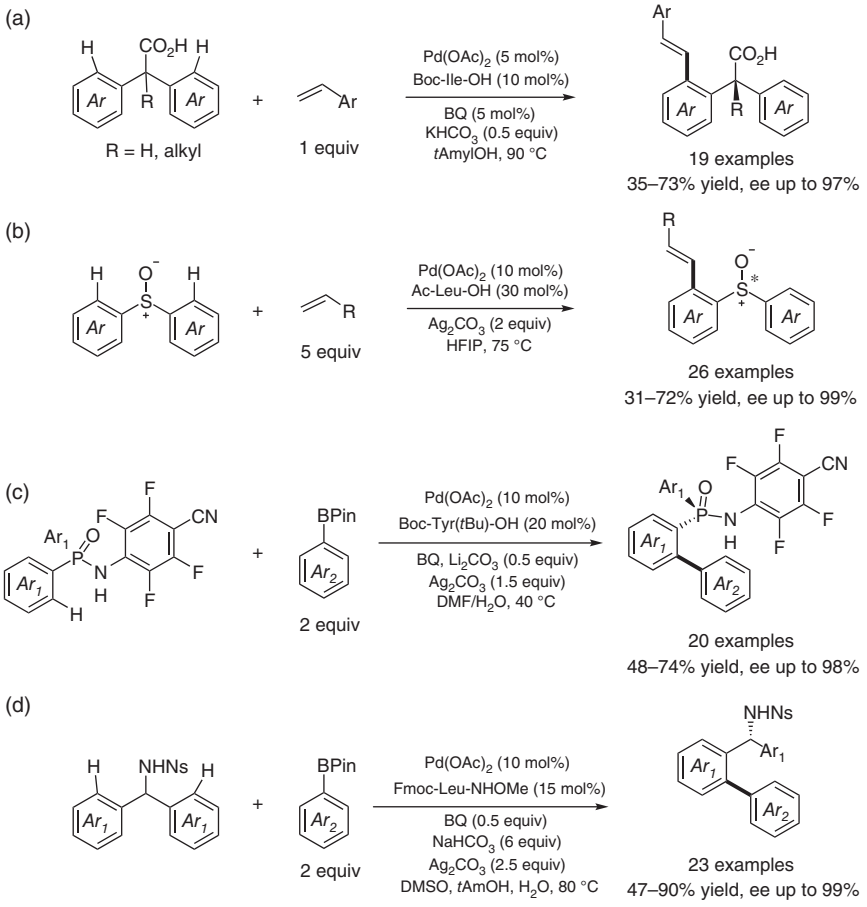

Scheme 3 Pd(II)-catalyzed desymmetrizing olefinations and arylations using MPAA ligands as chiral source in catalytic processes involving Pd(II)/Pd(0) redox cycles. Source: (a) Shi et al. [8]/American Chemical Society. (c) Du et al. [9]/American Chemical Society. (d) Laforteza et al. [10]/John Wiley & Sons.

Other common reactions used in desymmetrization processes with palladium catalysts and MPAA ligands are cross-couplings with aryl boron derivatives. Indeed, the group of Han used this methodology to build P-stereogenic phosphorus products via the desymmetrization of diarylphosphoramidites (Scheme 3c) [9]. The Yu group reported the arylation of nosyl-protected diarylmethylamines also using boronic esters (Scheme 3d) [10]. In this case, the best yields and enantioselectivities were obtained when the amino acids are used as methoxy amide derivatives.

Formal cycloaddition reactions are not very common in desymmetrization processes. In 2019, the group of Mascareñas and Gulías reported the desymmetrization of diarylmethylamines through a formal [4 + 2] cycloaddition with allenes. 2,6-F,F-Bz-Leu-OH was employed as a chiral source to build enantioenriched tetrahydroisoquinolines in excellent yields and enantioselectivities (Scheme 4a) [12]. The same substrates, but protected with a tosyl group, were used by the

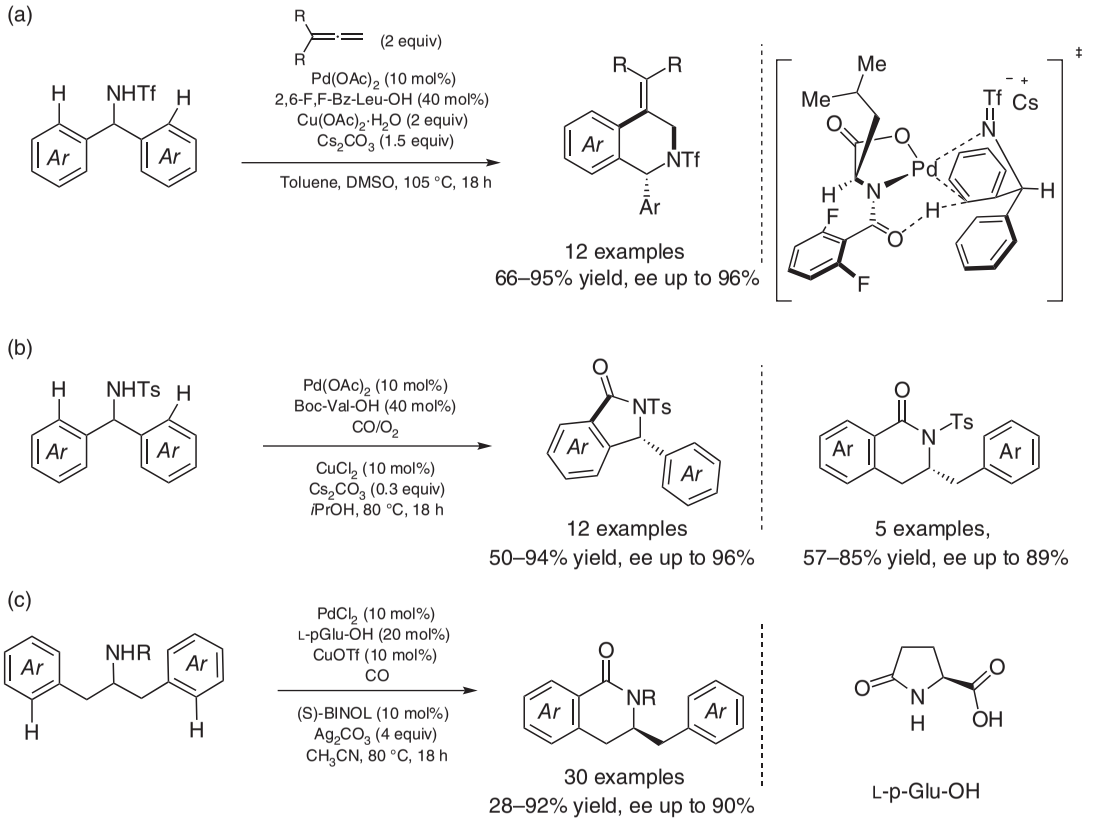

Scheme 4 Pd-catalyzed desymmetrizations of aromatic bonds using MPAA ligands and Pd(II)/Pd(0) redox cycles. Source: (a) Vidal et al. [12]/American Chemical Society. (b) Bai et al. [13]/American Chemical Society. (c) Han et al. [14]/American Chemical Society.

group of Xu for a carbonylation process to yield indolinones (Scheme 4b) [13]. The reaction is performed using a balloon containing a CO/O_2 atmosphere, and can also be extended to the synthesis of tetrahydroquinolones starting from the corresponding 1,3-diphenylpropan-2-amines. Almost simultaneously, Lan, Xia and coworkers reported another carbonylation process, in this case of alkyl-substituted diphenylpropan-2-amines, using L-pyroglutamic acid as chiral ligand (Scheme 4c) [14]. The use of (*S*)-1,1′-bi-2-naphthol (BINOL) as an additive allowed a significant increase in yields, although it has no impact in the enantioselectivity of the process. They also demonstrated that the products can be transformed into valuable compounds, such as chiral diimides.

The above-described desymmetrization reactions rely on Pd(II)/Pd(0) redox cycles, but related alternatives based on Pd(II)/Pd(IV) mechanisms have also been developed. The Yu group described pioneering examples of enantioselective lactonization of diphenylacetic acids, using phenyl iodoacetate as an oxidant promoting the formation of Pd(IV) intermediates (Scheme 5a) [15]. They also described asymmetric iodinations of diarylmethylamines with molecular iodine (Scheme 5b) [16].

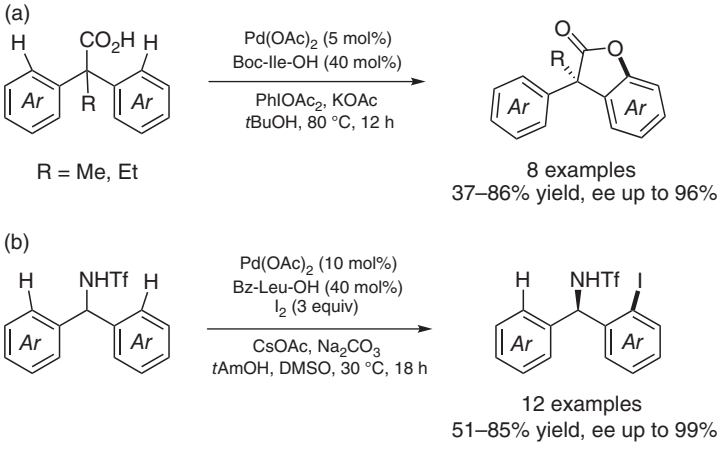

Scheme 5 Pd(II)-catalyzed desymmetrizations using MPAA ligands as chiral source relying on Pd(II)/Pd(IV) redox processes. Source: (a) Cheng et al. [15]/American Chemical Society. (b) Chu et al. [16]/American Chemical Society.

Aside from palladium, rhodium catalysts have also been used in desymmetrizing reactions, especially in formal cycloadditions. Therefore, Matsunaga and coworkers reported an asymmetric C—H alkylation of diarylmethylamines with diazomalonates assisted by chiral carboxylic acids (CCA). The functionalization is followed by cyclization and decarboxylation to afford 1,4-dihydroisoquinolin-3(2*H*)-ones (Scheme 6a) [17]. Cramer [18] and Li [19] groups independently published desymmetrizing annulations of sulfoximines with diazo compounds (Scheme 6b). In Cramer's work, the enantioselectivity is induced by an Rh(III) complex equipped with a chiral cyclopentadienyl ligand **(Rh1)**, and the selectivity is enhanced

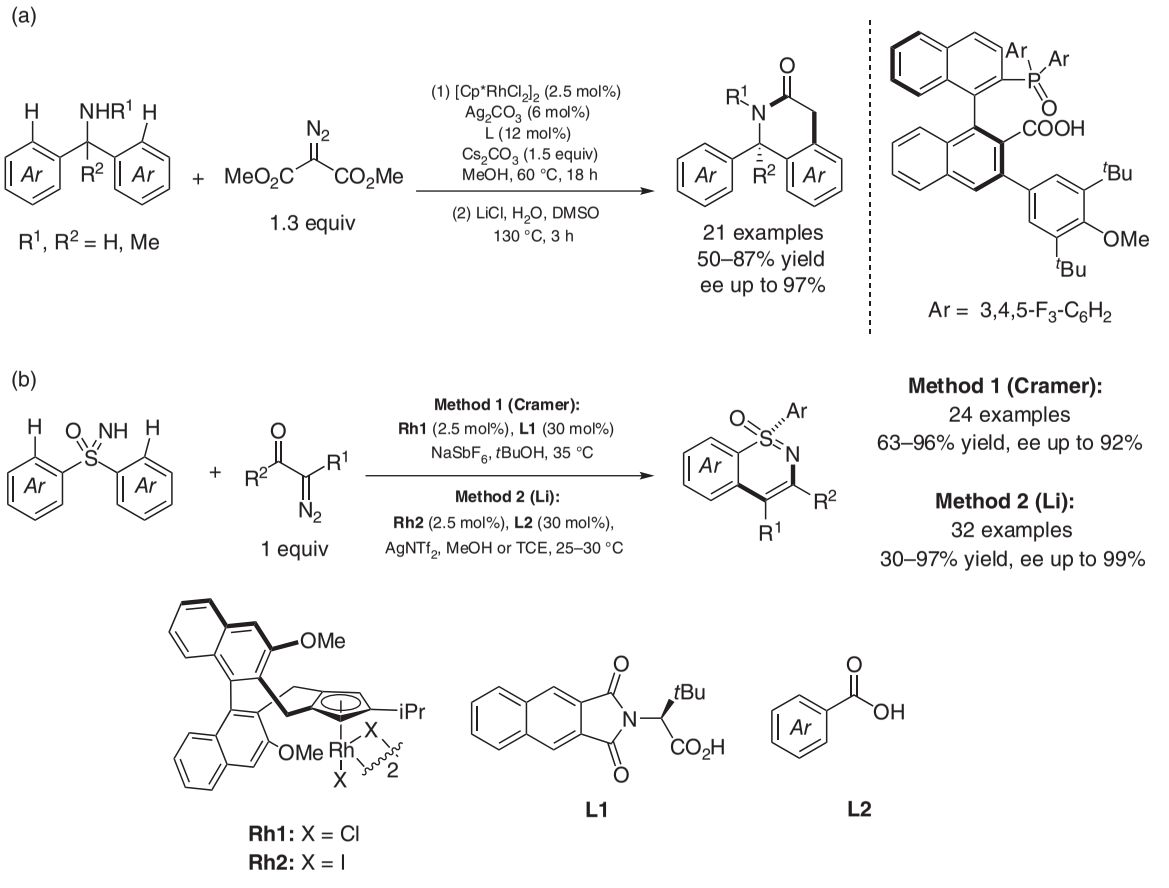

Scheme 6 Rh (III)-catalyzed desymmetrizations of diarylmethylamines and sulfoximines. Source: (a) Lin et al. [17]/John Wiley & Sons.

by the addition of *tert*-leucine derivatives (**L1**). Li's work also uses a related cyclopentadienyl rhodium complex (**Rh2**) and revealed a surprising effect of the carboxylic acid additive: it is possible to invert the enantioselectivity by simply switching from 2-methoxybenzoic to 2,6-dimethoxybenzoic acid.

Also using rhodium catalysts, Li et al. have recently published an enantio- and diastereoselective annulation of phosphinamides with diarylacetylenes by a twofold C—H activation, which provides for the synthesis of axially chiral biaryls. While the enantioselectivity derives from the rhodium catalyst (**Rh1**), the diastereoselectivity of the second C—H activation is under both remote and catalyst control (Scheme 7) [20].

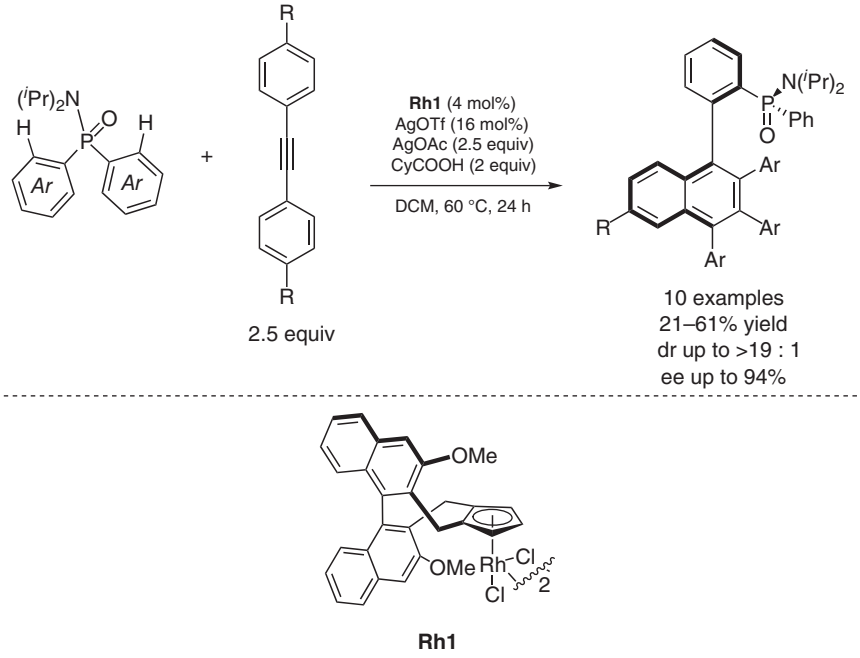

Scheme 7 Rh(III)-catalyzed desymmetrizations of phosphinamides based on a twofold C—H activation reported by Li and coworkers. Source: Li et al. [20]/John Wiley & Sons.

Cramer's group has also reported desymmetrizing C—H activations based on iridium catalysis, such as an iridium-catalyzed coupling of phosphine oxides with tosyl azide [21]. High enantioselectivities were achieved combining an iridium complex bearing a chiral cyclopentadienyl ligand (**Ir1**) with a chiral amino acid (*tert*-leucine derivative, **L3**). They found that yields and selectivities depend on the presence of match–mismatch effects. The same group reported that phosphorous oxides can also be desymmetrized under similar conditions for arylation reactions with *o*-quinone diazos (Scheme 8) [22].

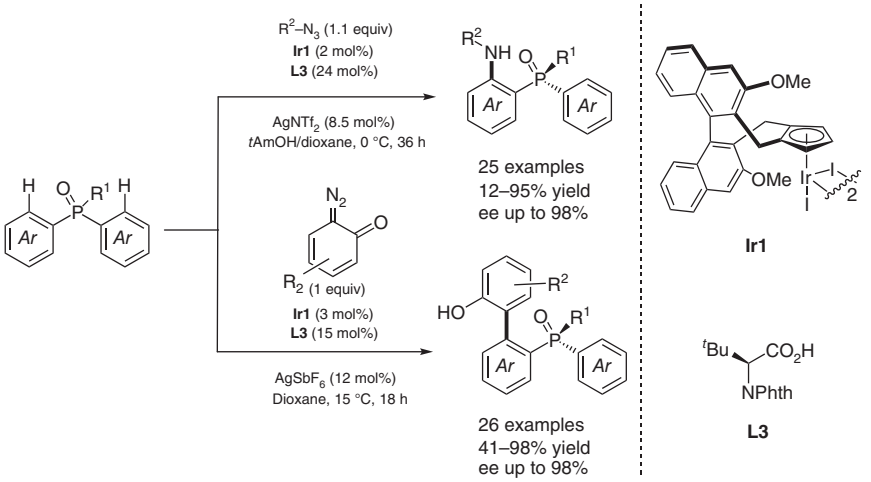

Scheme 8 Ir(III)-catalyzed desymmetrizations of phosphine oxides via amination or arylation reactions. Source: (a) Jang et al. [22]/John Wiley & Sons.

2.1.2 Activation of C(sp^3)—H bonds

The first example of a desymmetrizing reaction involving the activation of C(sp^3)—H bonds was reported by Yu's group in 2008, as a part of a larger study concerning enantioselective C(sp^2)—H activations (see Section 2.1.1) [7]. They described an asymmetric butylation of 2-isopropylpyridine through a palladium-catalyzed enantioselective C(sp^3)—H activation assisted by a cyclopropyl α-amino acid ligand (**L4**) (Scheme 9a). In general, the desymmetrization of acyclic alkyl chains is highly challenging, and there are few precedents. Yu's group achieved moderate success in the asymmetric arylation of carboxyamides bearing prochiral quaternary α-carbons using hydroxamic acids as palladium ligands (**L5**) (Scheme 9b) [23]. They also performed related borylation reactions using acetyl-protected aminomethyl oxazolines (APAO, **L6**) as chiral ligands (Scheme 9c) [24].

Yu and coworkers have also reported several examples of desymmetrizing reactions of prochiral cyclopropyl and cyclobutyl carboxylic acids [25] (Scheme 10a). These reactions generate products with two stereocenters, as in addition to the loss of point symmetry, there is an asymmetric functionalization of a methylene group. These reactions also involve the use of palladium catalysts (Pd(II)/Pd(0) redox cycles) and MPAAs (**L7**) or diamine ligands (MPAAM, **L8**) as chiral inductors. Cyclopropyl [26] and cyclobutyl [23] amide derivatives can also be arylated using organoboron compounds as coupling partners and MPAAs (**L9**) or mono-protected α-amino-*O*-methyl hydroxamic acids (MPAHA, **L10**) as chiral ligands (Scheme 10b). In addition such substrates can also be borylated using acetyl-protected aminomethyl oxazolines (APAO, L11) ligands (Scheme 10c) [24].

The enantioselective modification of C(sp^3)—H bonds can also be achieved relying on mechanisms that involve Pd(II)/Pd(IV) redox cycles (Scheme 11). Thus, the Yu lab has reported the arylation, alkenylation, and alkynylation of isobutyramides with

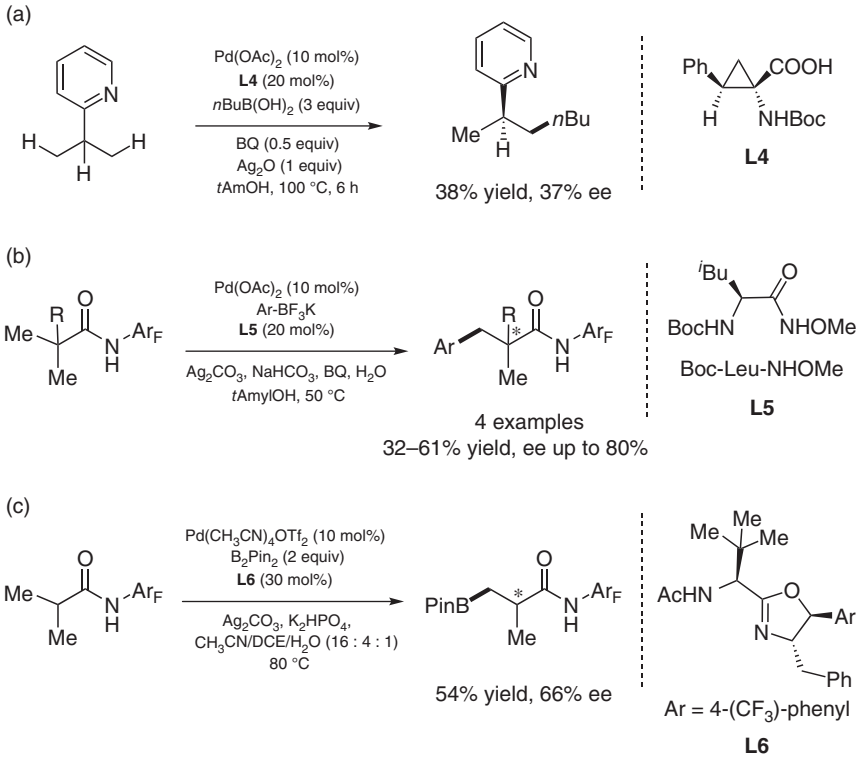

Scheme 9 Pd(II)-catalyzed desymmetrizations of acyclic C(sp^3)—H bonds via Pd(II)/Pd(0) catalytic cycles. Source: (b) Xiao et al. [23]/American Chemical Society. (c) He et al. [24]/American Chemical Society.

the corresponding iodo derivatives to give products with enantiomeric excesses up to 98% (Scheme 11) [27].

The same strategy can also be used for the MPAA-accelerated Pd-catalyzed asymmetric C(sp^3)—H arylation of cyclopropyl amine, triflamide, or carboxylic acid derivatives (Scheme 12a–c) [28–30], using aryl iodides as coupling partners.

In addition to simple functionalizations, it is possible to achieve desymmetrizing cyclizations based on the activation of C(sp^3)—H bonds. Therefore, Gaunt and coworkers reported interesting aminocyclizations in designed dimethylated amino acid derivatives, using a Pd catalyst and an anionic BINOL–phosphoric acid as chiral ligand. The reaction produces chiral aziridines (Scheme 13) [31].

There are very few publications on related asymmetric activations of C(sp^3)—H bonds using other transition metal-based catalysts than Pd. In 2021, Liu, Chang, Li, and coworkers disclosed a C(sp^3)—H amidation of prochiral oxime ethers with iodonium imides using a chiral rhodium complex (Scheme 14a) [32]. After the C—H activation, the reaction entails the formation of an Rh(V)–nitrene intermediate, which evolves by migratory insertion and protonolysis to give the enantioenriched amidation product. The same year, Lin, Yoshino, Matsunaga,

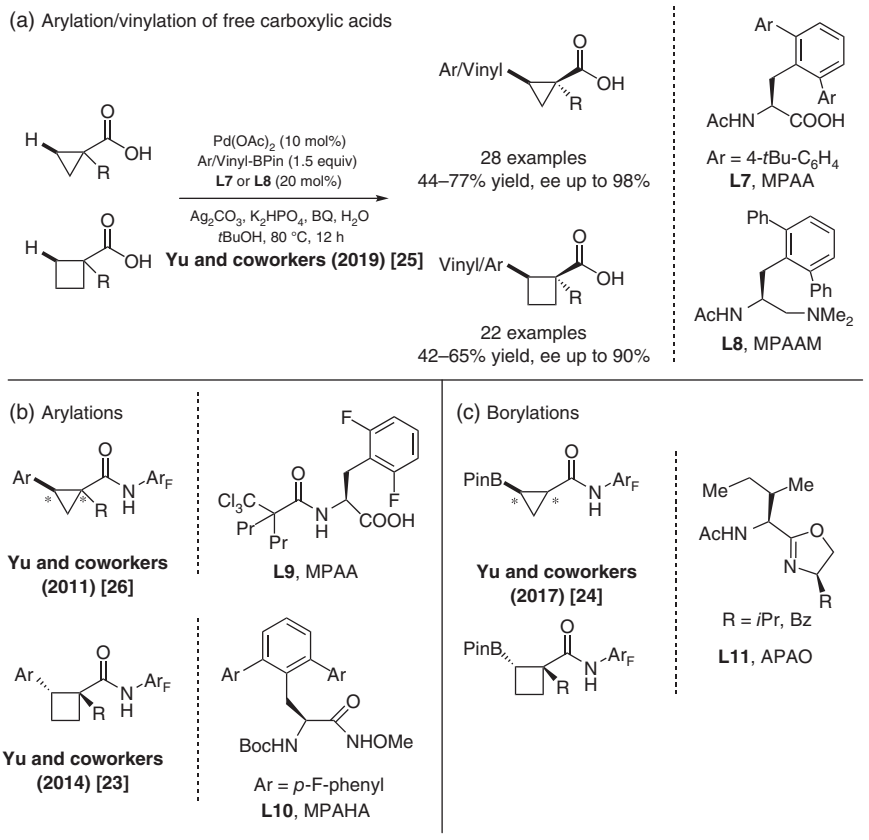

Scheme 10 Pd(II)-catalyzed desymmetrization of cyclic C(sp^3)—H bonds via Pd(II)/Pd(0) catalytic cycles reported by Yu and coworkers.

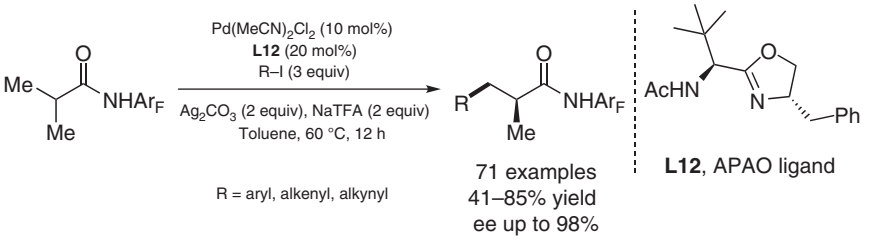

Scheme 11 Pd(II)-catalyzed desymmetrization of acyclic C(sp^3)—H bonds via Pd(II)/Pd(IV) catalytic cycles reported by Yu and coworkers. Source: Wu et al. [27]/American Association for the Advancement of Science.

and coworkers reported a desymmetrizing C(sp^3)—H amidation of 2-alkylpyridine derivatives with dioxazolones (Scheme 14b). The combination of a rhodium catalyst with a pseudo-C_2-symmetric CCA exhibiting a binaphthyl backbone allowed the formation of the amidated products with ees up to 92% [33].

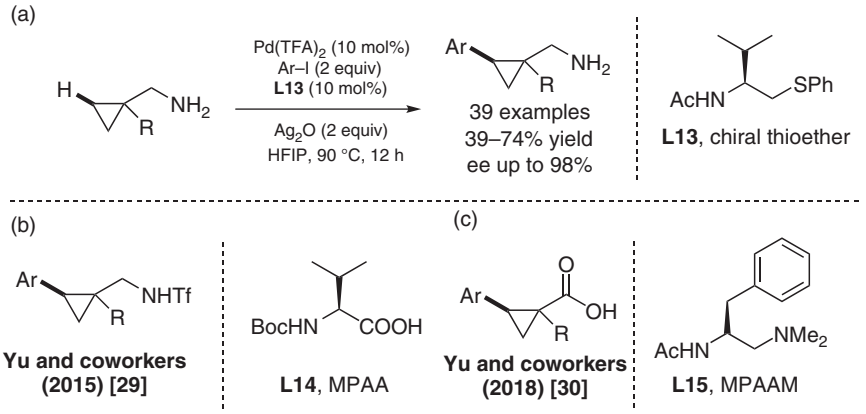

Scheme 12 Pd(II)-catalyzed desymmetrizations of cyclic C(sp^3)—H bonds via Pd(II)/Pd(IV) catalytic cycle reported by Yu and coworkers. Source: (a) Zhuang and Yu [28]/Springer Nature.

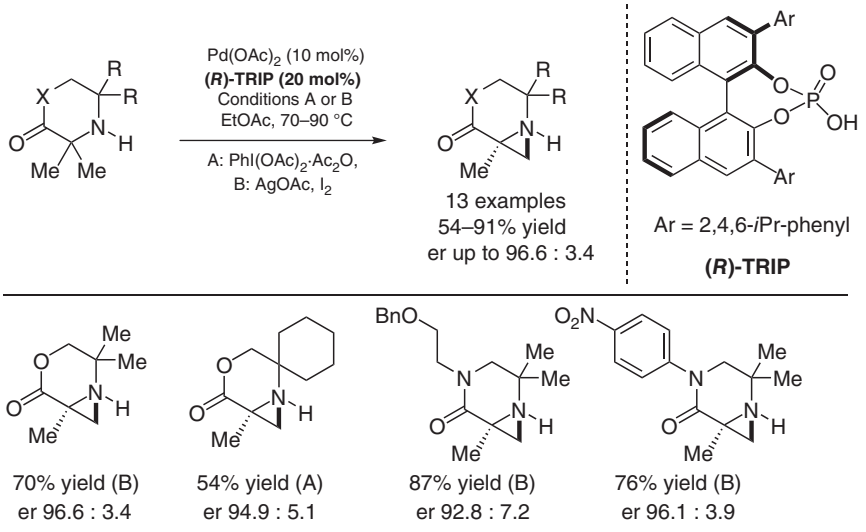

Scheme 13 Pd(II)-catalyzed desymmetrizing aminocyclization. Source: Shen et al. [31]/American Chemical Society.

2.2 Reactions Initiated by Oxidative Additions of C—X Bonds

One strategy to indirectly activate C—H bonds involves the *in situ* generation of the required electrophilic metal species by oxidative addition of a C—X bond of the substrate to a low-valent transition metal. This type of activation has been essentially restricted to palladium catalysis.

2.2.1 Activation of C(sp^2)—H Bonds

The first article using the above approach was published by Cramer and coworkers in 2009 [34] and deals with the intramolecular desymmetrizing C—H arylation of vinyl

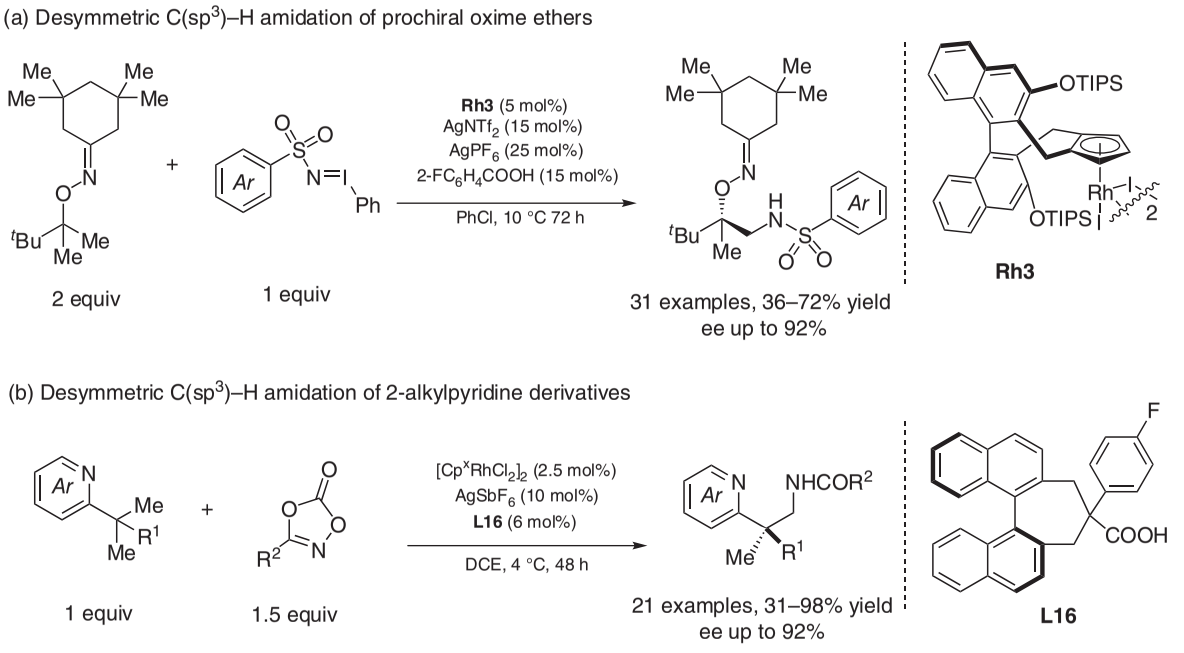

Scheme 14 Rh(III)-catalyzed desymmetrizing C(sp^3)—H amidations of β-amino alcohols and 2-alkylpyridine derivatives. Source: (a) Liu et al. [32]/John Wiley & Sons.

triflates. The reactions that use α,α,α′,α′-tetraaryl-1,3-dioxolane-4,5-dimethanol (TADDOL)-derived phosphoramidites as chiral ligands (**L17**) allow the formation of chiral indanes bearing a quaternary stereocenter (Scheme 15a). These types of monodentate ligands were also used for the synthesis of dibenzazepinones from *N*-acyl-2-bromoanilines in a follow-up paper published by the same group (Scheme 15b) [35].

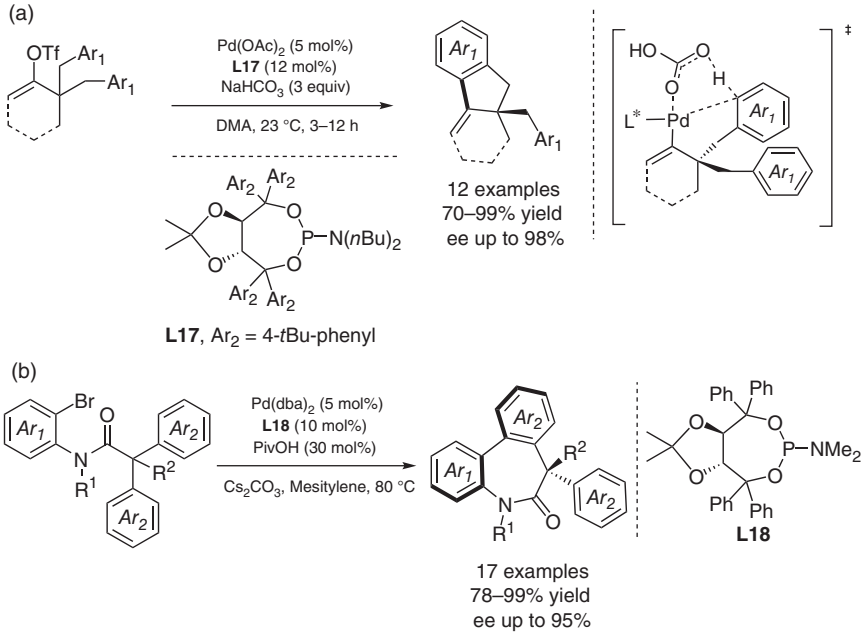

Scheme 15 Pd(0)-catalyzed intramolecular desymmetrizing C(sp^2)—H arylations assisted by TADDOL-derived phosphoramidite ligands and proposed transition states. Source: (b) Saget and Cramer [35]/John Wiley & Sons.

Phosphoramidites have also been used as chiral ligands in the palladium-catalyzed asymmetric intermolecular imidoylation of dibenzyl isocyanides, as reported by Zhu, You, and coworkers. The reaction is initiated in the isonitrile group, to give a Pd(II) species that is responsible for the C—H activation (Scheme 16), and provides rapid access to valuable dihydroisoquinolines containing a chiral quaternary center (up to 92% enantiomeric excess) [36].

Besides, Duan and coworkers [37] and Liu, Ma, and coworkers [38] concurrently reported an intramolecular desymmetrizing C—H arylation of prochiral phosphinic amides equipped with a bromoaryl substituent for the synthesis of P-stereogenic products (Scheme 17). These reactions use TADDOL-based phosphoramidite ligands for the chiral induction (**L20**, **L21**).

Similar asymmetric processes can also be induced using other types of chiral monodentate ligands. Thus, the Tang's group disclosed a desymmetrizing intramolecular arylation of diaryl 2-bromo arylphosphonate precursors, using palladium catalysts

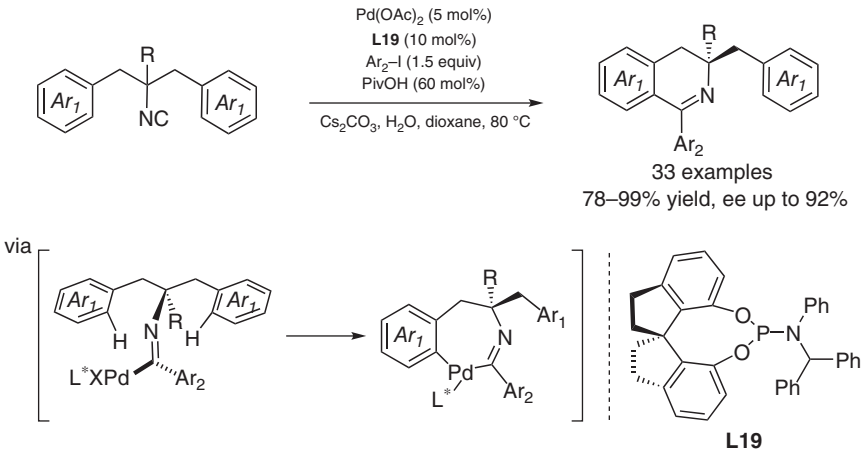

Scheme 16 Pd(0)-catalyzed intermolecular desymmetric C(sp^2)—H imidoylation of dibenzyl isocyanides. Source: Zhu and coworkers.

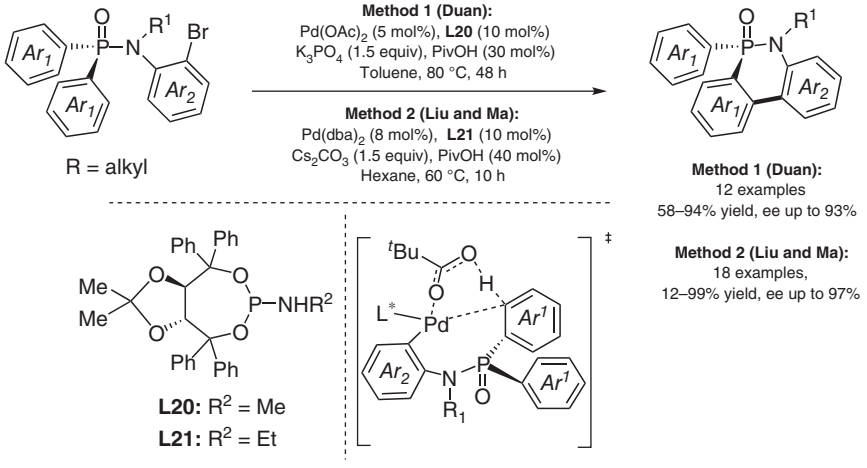

Scheme 17 Pd(0)-catalyzed intramolecular desymmetric C(sp^2)—H arylations of prochiral phosphinic amides.

and P-chiral phosphine ligands [39]. Cramer and coworkers reported an asymmetric C—H intramolecular arylation of ketene aminal phosphates with the aid of their newly developed phospholane-type of ligand that possesses both axial and point chirality (Scheme 18) [40].

Bidentate, chiral phosphine ligands have also been successfully used in several desymmetrizing intramolecular arylations triggered by low-valent transition metals (Scheme 19). Shintani, Hayashi, and coworkers described an efficient enantioselective C—H arylation of prochiral 2-(arylsilyl)aryl triflates using electron-rich Josiphos-type palladium ligands (**L23**) [41]. Cui, Xu, and coworkers disclosed a related C—H arylation of *o*-bromoaryl phosphine oxides for the

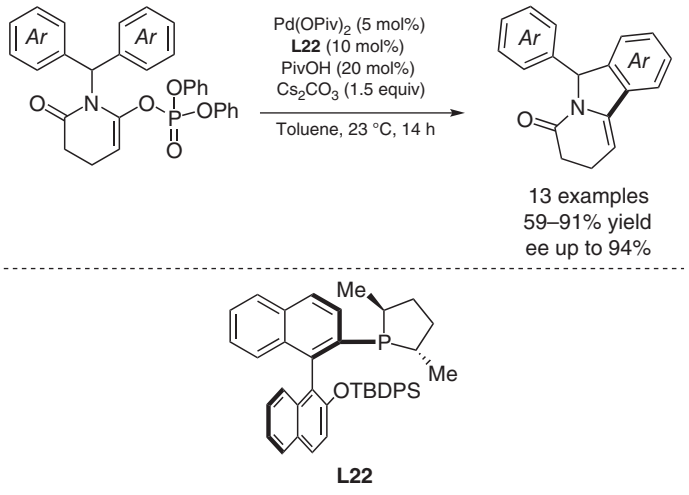

Scheme 18 Pd(0)-catalyzed intramolecular desymmetrizing C(sp^2)—H arylations assisted by a phospholane-type ligand developed by Cramer and coworkers. Source: Grosheva and Cramer [40]/American Chemical Society.

synthesis of P-stereogenic dibenzophospholes [42]. Two years later, Duan and coworkers described a similar process using (*R*)-SegPhos rather than (*S,S*)-1,2-bis(2,5-dimethylphopholano)benzene ligands, which showed a higher functional group tolerance [43].

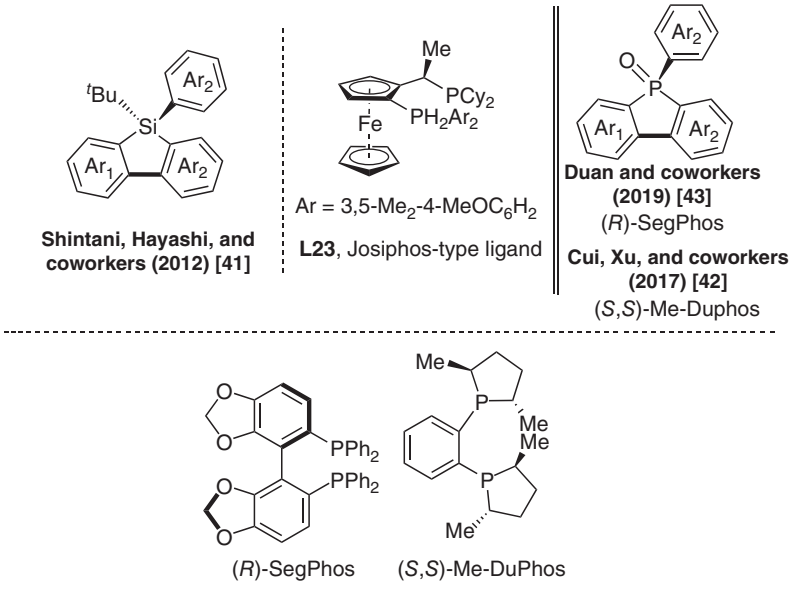

Scheme 19 Pd(0)-catalyzed intramolecular desymmetric C(sp^2)—H arylations assisted by chiral bidentate phosphines.

In 2018, Baudoin and coworkers published elegant asymmetric intramolecular arylations, also based on Pd(0)/Pd(II) catalytic cycles, but using a bifunctional ligand (**L24**) containing both a phosphine and a carboxylate unit that assists the C—H activation step [44]. The presence of both groups is essential for obtaining high enantioselectivities (Scheme 20).

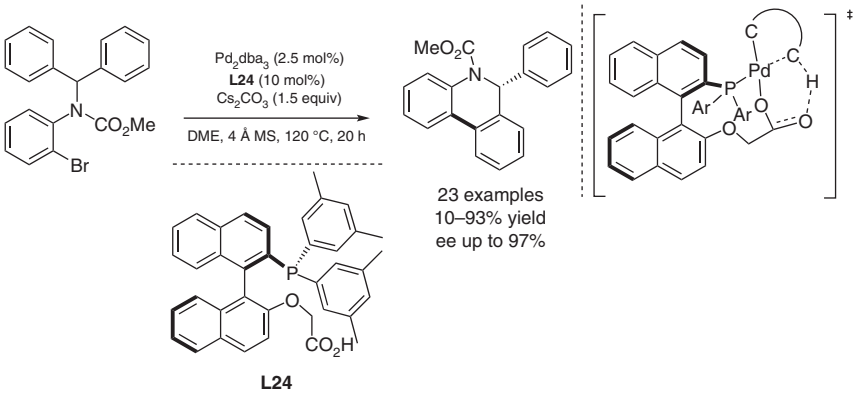

Scheme 20 Pd(0)-catalyzed intramolecular desymmetrizing C(sp^2)—H arylations assisted by a bifunctional chiral ligand.

2.2.2 Activation of C(sp^3)—H Bonds

The above-described mechanistic approach to activate C—H bonds after an initial oxidative addition has been shown particularly successful in desymmetrization reactions that engage C(sp^3)—H bonds, mainly in cyclization processes, as in the case of their sp^2 counterparts.

The first example on the use of this methodology for desymmetrizing prochiral methyl groups was published in 2011 by Kagan and coworkers [45] in the synthesis of 2-methyl indolines from 2-halo-*N*-isopropyl anilides (Scheme 21a). The process is catalyzed by palladium acetate and uses Me-DUPHOS as chiral ligand. A related cyclization was later developed by Baudoin and coworkers using a chiral phosphate as catalytic base and an achiral tricyclohexylphosphine ligand (Scheme 21b) [46, 47]. The reaction presents a broad scope, and the enantioselectivities were slightly higher than in the Kagan's work. The cyclization of related *N*-(*o*-Br-aryl) amides was later described by Duan and coworkers in the formation of quaternary α-nitro lactams (Scheme 21c) [48]. In this case, a TADDOL-based phosphoramidite (**L25**) was found optimal for the asymmetric induction.

This type of asymmetric processes are not limited to the activation of methyl groups. In fact, Kündig and coworkers reported in 2011 a carbocyclization entailing the activation of C(sp^3)—H bonds of cyclohexyl groups that affords chiral fused indolines. The reaction is promoted by Pd catalysts and chiral *N*-heterocyclic carbene-type ligands (**L26**) (Scheme 22a) [49]. The mechanism and scope of this reaction was further studied in a follow-up paper published by the same group [53]. In 2012, Cramer and coworkers disclosed a similar entry to fused indolines from

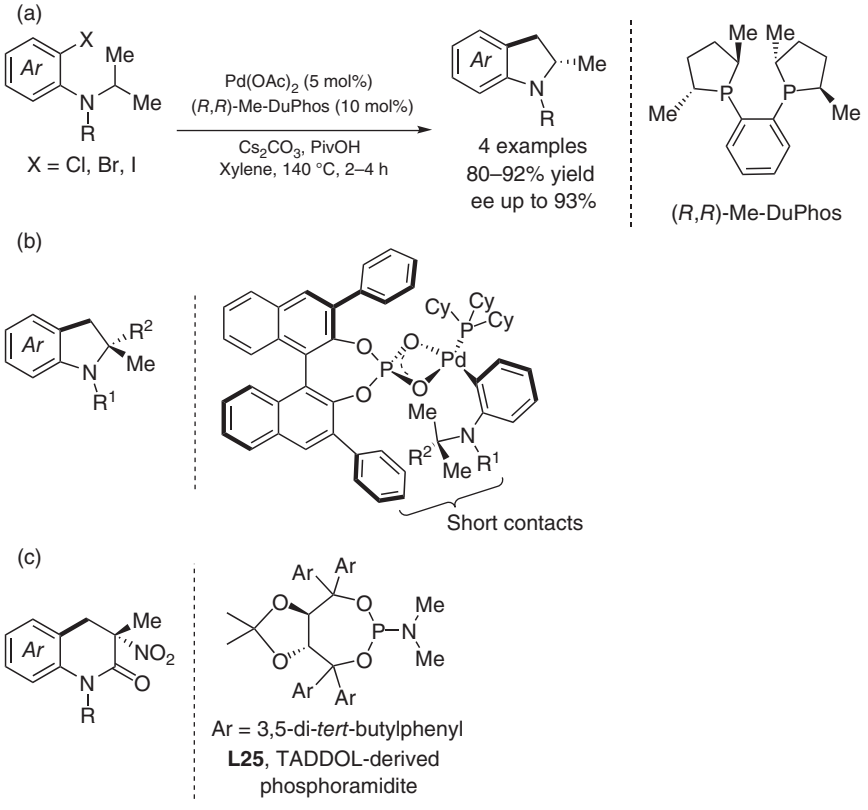

Scheme 21 Pd(0)-catalyzed intramolecular desymmetric C(sp^3)—H arylations for the synthesis of azaheterocycles. Source: (b) Adapted from Yang et al. [46] and Melot et al. [47]. (c) Kong et al. [48]/Royal Society of Chemistry.

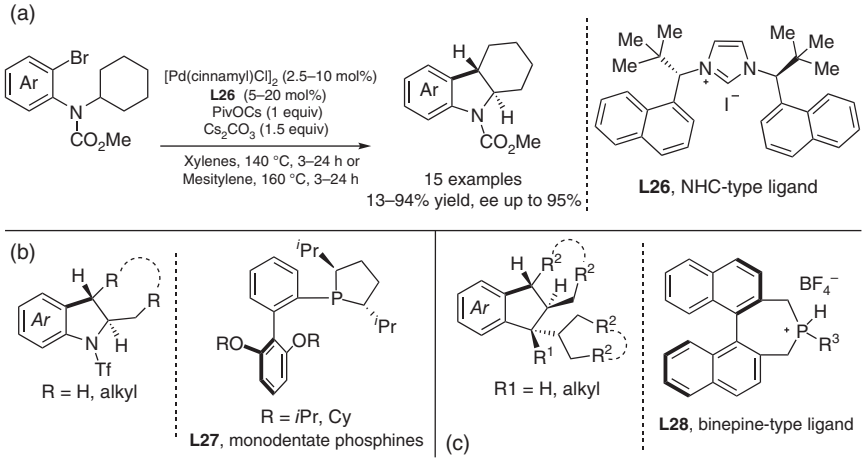

Scheme 22 Pd(0)-catalyzed intramolecular desymmetric C(sp^3)—H arylations in cyclic precursors. Source: (a) Nakanishi et al. [49]/John Wiley & Sons. (b) Saget et al. [50]/John Wiley & Sons. (c) Adapted from Martin et al. [51] and Holstein et al. [52].

aryl triflates using chiral monodentate phosphines (**L27**) as asymmetric inductors (Scheme 22b) [50]. Binepine ligands (**L28**) were found by Baudoin and coworkers to be excellent chiral ligands in a related carbocyclization process of aryl bromides to give fused cyclopentanes (Scheme 22c) [51, 52].

The methylene group of cyclopropyl rings can also be activated using a Pd-promoted process to give strained bicycles such as those shown in Scheme 23. Cramer and coworkers demonstrated the viability of the methodology using TADDOL-derived phosphoramidite ligands (**L26**) and triflyl-protected anilines as precursors (Scheme 23a) [54]. This method was complemented with a follow-up paper published by the same group in which they expanded the scope to assemble dihydroquinolones and dihydroisoquinolones (Scheme 23b) [55]. They also

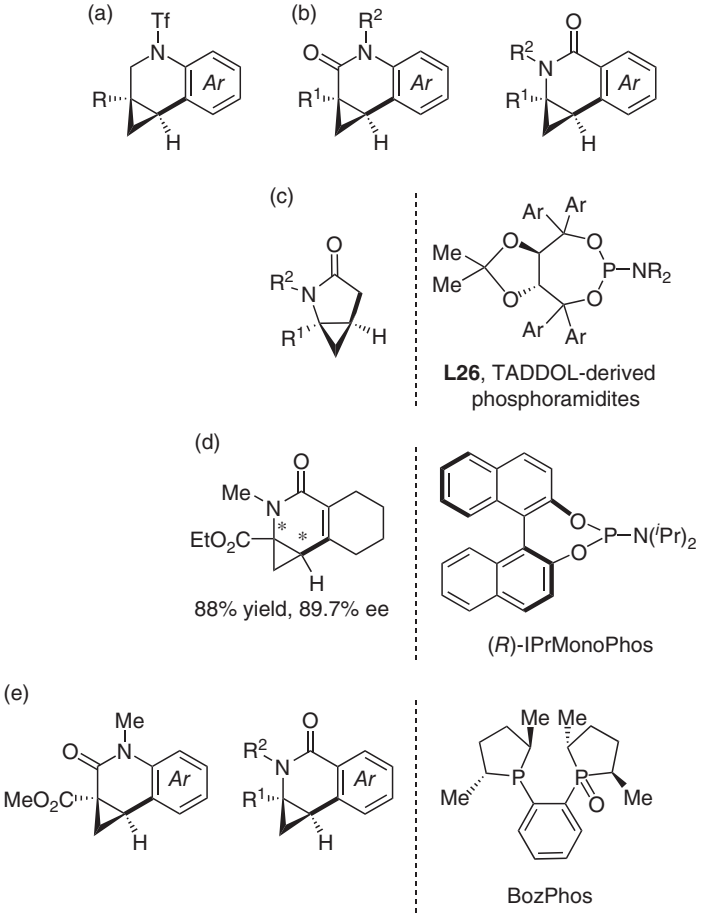

Scheme 23 Pd(0)-catalyzed intramolecular desymmetric C(sp^3)—H arylations of cyclopropanes with the aid of phosphoramidites and BozPhos ligands. Source: (a) Saget and Cramer [54]/John Wiley & Sons. (b) Pedroni et al. [55]/Royal Society of Chemistry. (c) Pedroni and Cramer [56]/John Wiley & Sons. (d) Ladd and Charette [57]/American Chemical Society. (e) Mayer et al. [58]/American Chemical Society.

developed a desymmetrizing C(sp^3)—H cyclization of chloracetamides to access γ-lactams (Scheme 23c) [56].

Inspired by this work, Charette and coworkers explored BINOL-derived phosphoramidite (*R*)-IPrMonophos and BozPhos bidentate ligands in related alkenylation reactions instead of arylation processes, obtaining moderate to good ees (Scheme 23d) [57]. In 2019, they published an article demonstrating the efficiency of BozPhos ligands in Cramer's reaction (synthesis of dihydroquinolones and dihydroisoquinolones, Scheme 23e) [58].

2.3 Reactions Initiated by Oxidative Addition of C—H Bonds to Low-valent Transition Metals

The activation of C—H bonds to give metalated derivatives can also be promoted by direct oxidative addition to low-valent transition metals. If the metal reagent contains chiral ligands, the transformation can be used to desymmetrize prochiral precursors. This strategy has been demonstrated especially for rhodium and iridium catalysts, rather than palladium, owing to their inherent ability to undergo such oxidative additions [59].

2.3.1 Activation of C(sp^2)—H Bonds

In 2013, Takai, Kuninobu, and coworkers reported the enantioselective synthesis of chiral spirosilabifluorene derivatives from bis(biaryl) silanes through a rhodium-catalyzed double dehydrogenative cyclization, using (*R*)-2,2′-bis(diphenylphosphino)-1,1′-binaphthalene) (BINAP) as ligand (Scheme 24a) [60]. In a related process initiated by an oxidative addition of (hydrido)silyl ether precursors, Hartwig and coworkers disclosed in 2015 a rhodium-catalyzed desymmetrizing C—H silylation of benzophenone derivatives (Scheme 24b) [61]. The reaction starts by dehydrogenative formation of a silicon metal bond followed by activation of the aromatic C—H bond by oxidative addition and reductive elimination to give the final chiral silylacycle. The best results were obtained using Walphos (**L27**) or catASium (**L28**) ligands, depending on the substrate. Two years later, the same group reported the iridium-catalyzed version of the reaction using pyridinyl-oxazoline-type ligands (**L29**) (Scheme 24c) [62]. In a related process, the same group published a iridium-catalyzed desymmetrizing C—H borylation of diarylmethyl silanes (Scheme 24d) [63]. In 2019, the group of Ke and Xu reported an iridium-catalyzed enantioselective borylation of prochiral diarylmethylamines through a free amine-directed desymmetrizing oxidative addition (Scheme 24e) [64]. In this reaction, the enantioselectivity is induced by a chiral pyridylboryl ligand (**L30**).

In the context of this chemistry, it is worth highlighting the iridium-catalyzed desymmetrizing remote C—H borylation reported by the group of Phipps [65] (Scheme 25). In these reactions the mechanism proposed for the enantioinduction lies on the electrostatic interactions with a chiral cation (**L31**).

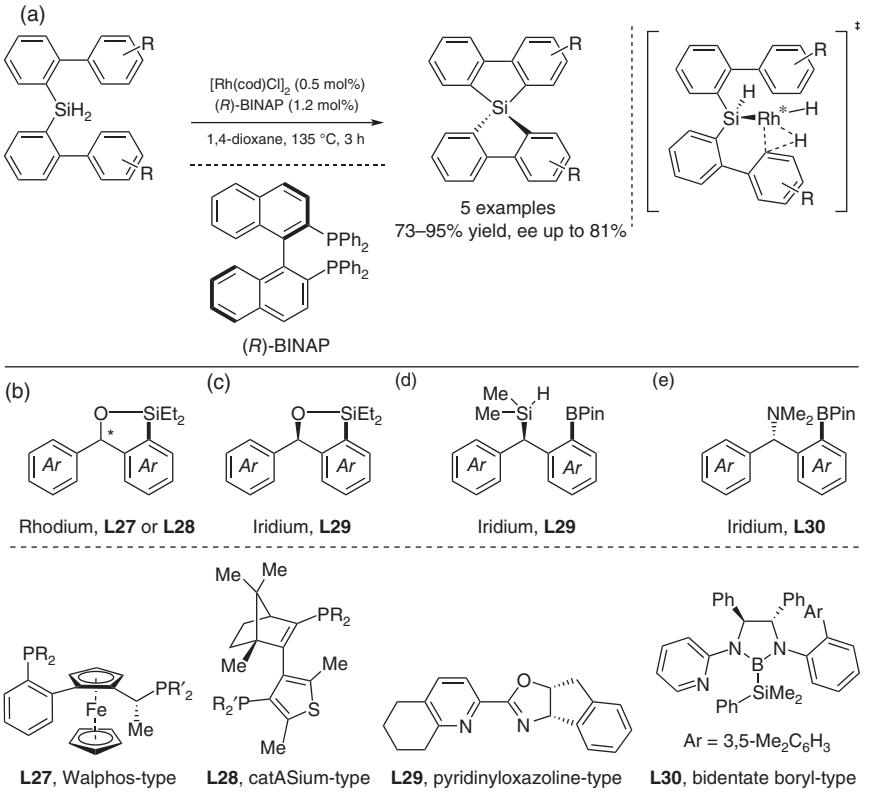

Scheme 24 Rhodium- and iridium-catalyzed desymmetric C(sp^2)—H functionalizations based on a C—H oxidative addition strategy and the proposed transition state. Source: (a) Kuninobu et al. [60]/John Wiley & Sons. (b) Lee et al. [61]/American Chemical Society. (c, d) Su et al. [62, 63]/John Wiley & Sons. (e) Zou et al. [64]/American Chemical Society.

2.3.2 Activation of C(sp^3)—H Bonds

There are very few reports on desymmetrizing C(sp^3)—H activations triggered by direct oxidative additions of C—H bonds to transition metals, and all of them consist of intramolecular silylations (Scheme 26). In 2015, Murai et al. described the asymmetric synthesis of dihydrobenzosiloles from the corresponding acyclic silyl hydrides, using rhodium catalysis and (*R*)-5,5′-bis[di(3,5-di-*tert*-butyl-4-methoxyphenyl)phosphino]-4,4′-bi-1,3-benzodioxole (DTBM-SegPhos) as chiral ligand [66]. This protocol was complemented by the work of the Hartwig group that, published in 2017 an iridium-catalyzed version of this reaction using chiral pyridyloxazolines (**L29**) as ligands [67]. In 2016, Hartwig and coworkers described a rhodium-catalyzed intramolecular desymmetrizing silylation of cyclopropanes employing (*S*)-DTBM–SegPhos as chiral ligand. The reaction constitutes the first catalytic, enantioselective functionalization of a C—H bond in a cyclopropane to form a carbon–silicon bond [68].

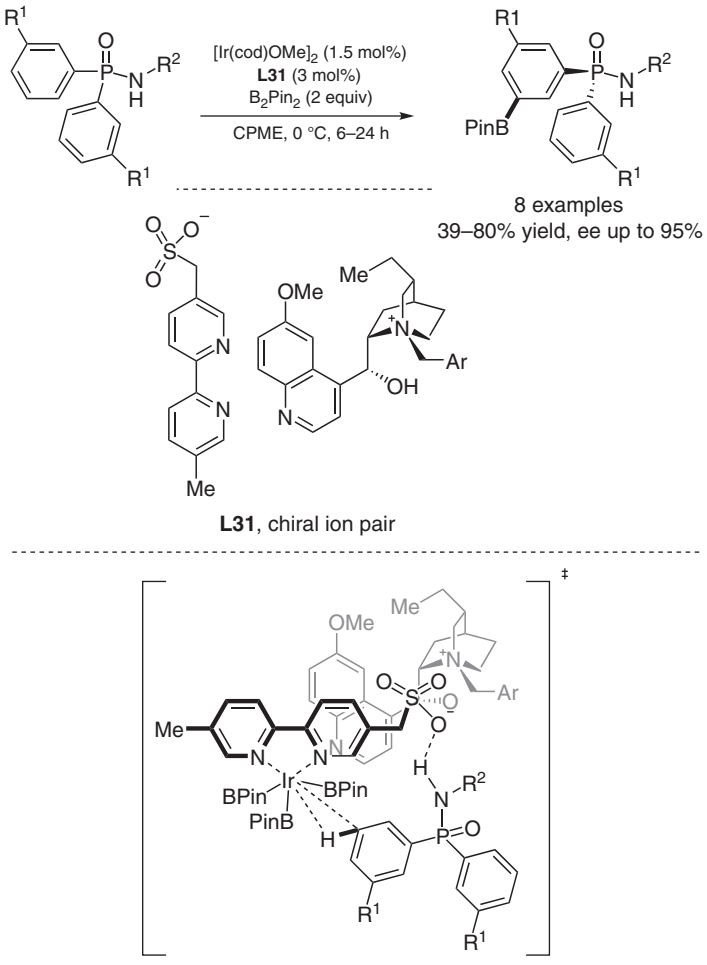

Scheme 25 Iridium-catalyzed desymmetric remote C(sp^2)—H borylations directed by a chiral cation reported by Phipps and coworkers and the proposed transition state. Source: Genov et al. [65]/American Association for the Advancement of Science.

3 Desymmetrizations Generating Axial Chirality

The atroposelective functionalization of C—H bonds has emerged as a powerful strategy to introduce *ortho* substituents in fluxional biaryl moieties [69, 70]. In these transformations, the added functionality blocks the rotation of the biaryl axis, resulting in products with axial chirality. Depending on the rotation barriers around the prostereogenic axis of the biaryl, the interconverting atropoisomeric precursors can be considered as either racemic mixtures or achiral compounds. The values of these rotation barriers are rarely known, which brings controversy on whether these reactions are desymmetrizations of fluxional biaryls or dynamic kinetic

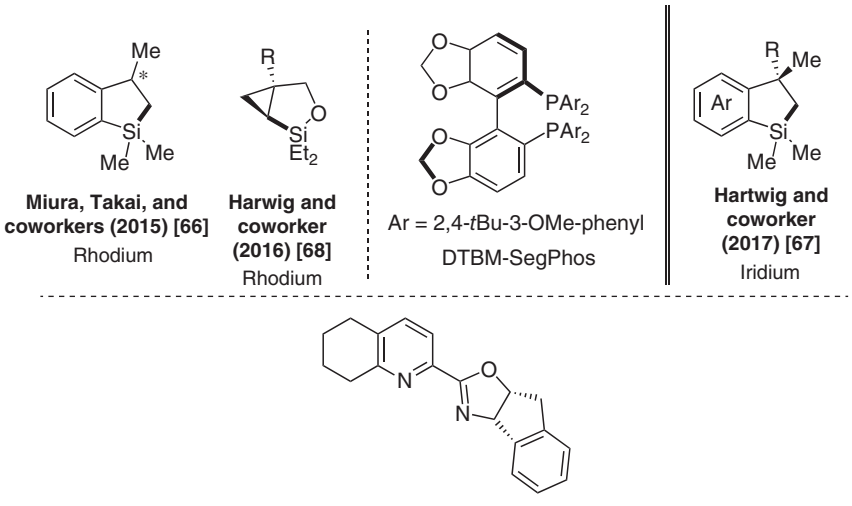

Scheme 26 Examples of desymmetrizing C(sp^3)—H silylations by direct oxidative addition of C—H bonds.

resolutions. In this article, in the cases where the rotation barrier is low, or there is no information on it, we have considered these processes as desymmetrizations. It is important to note that in most cases there is no mechanistic data to fully support the C—H activation as the enantiodetermining step.

3.1 Reactions Catalyzed by Electrophilic Transition Metal Complexes

The first examples reporting transition metal-catalyzed direct atroposelective functionalization of biaryl scaffolds leading to enantioenriched products consisted in C—H alkenylation processes. The You group reported in 2014 that Rh(III) catalysts featuring Cramer-type chiral C_2-symmetric Cp ligands [71] catalyzed the enantioselective dehydrogenative Heck-type coupling of 1-(naphthalene-1-yl)benzo[*h*] isoquinolines with ethylene, styrenes, or acrylates (Scheme 27) [72].

The application of these chiral Rh(III) catalysts has been extended to other atroposelective processes, based on enantioselective C—H activations [20, 73] and other C—H functionalizations where the C—H activation step is not enantiodetermining [74].

The You group, in 2016, devised a new class of chiral Rh catalysts bearing Cp ligands based on an axially chiral 1,1′-spirobiindane skeleton (**Rh5**) [75] and their use, with or without CCA additives, to perform enantioselective alkenylations of 1-(naphthalene-1-yl)benzo[*h*]isoquinoline cores [75]. The method was also used for dehydrogenative heteroarylations [76] as well as for annulation processes to give azoniahelicenes [77] (Scheme 28).

Pd catalysts can also be used for atroposelective C—H alkenylation and alkynylation reactions. Therefore, dehydrogenative Heck-type coupling of biaryl-containing

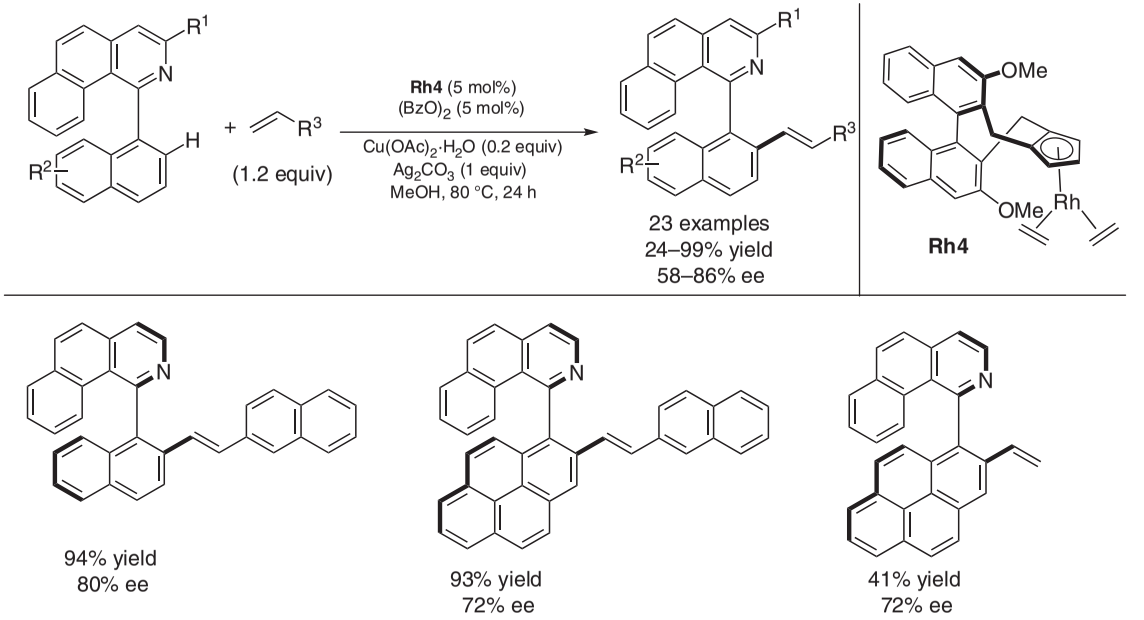

Scheme 27 Rh(III)-catalyzed atroposelective dehydrogenative Heck coupling between 1-(naphthalene-1-yl)benzo[*h*]isoquinoline cores architectures and alkenes. Source: Zheng and You [72]/John Wiley & Sons.

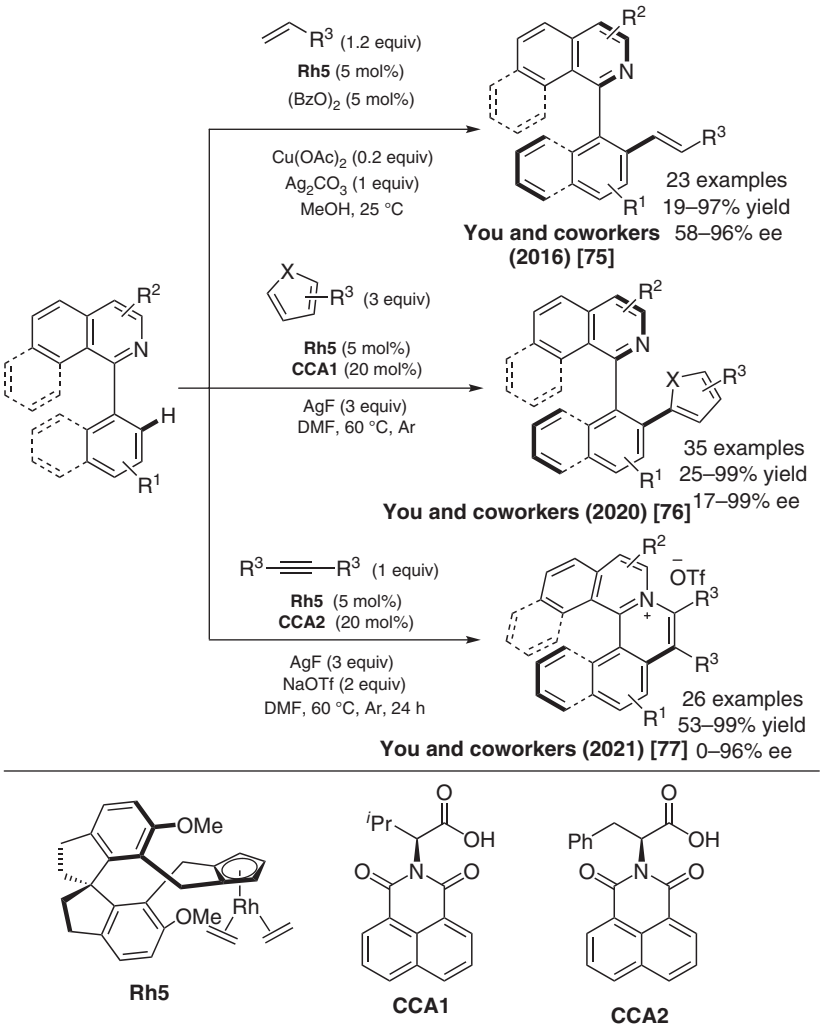

Scheme 28 Rh(III)-catalyzed atroposelective dehydrogenative couplings of 1-(naphthalene-1-yl)benzo[*h*]isoquinoline architectures using a Cp^{x}Rh catalyst bearing a spirobiindane core.

phosphine oxides with acrylates can be performed using Pd(II) catalysts and MPAA ligands, although the products were generally obtained with modest ees (Scheme 29) [78]. In 2020, Hong, Shi, and coworkers reported a method for the Pd(II)-catalyzed enantioselective alkenylation and alkynylation of styrenes equipped with pyridine-directing groups (Scheme 29) [79]. Crucial for the success of this highly atroposelective reaction is the use of L-pyroglutamic acid as ligand, which provided high for obtaining high ees. Indeed, density functional theory (DFT) studies demonstrated that the formation of one of the two possible palladacyclic enantiomers is favored by 4.5 kcal mol^{-1} difference, confirming an atroposelective

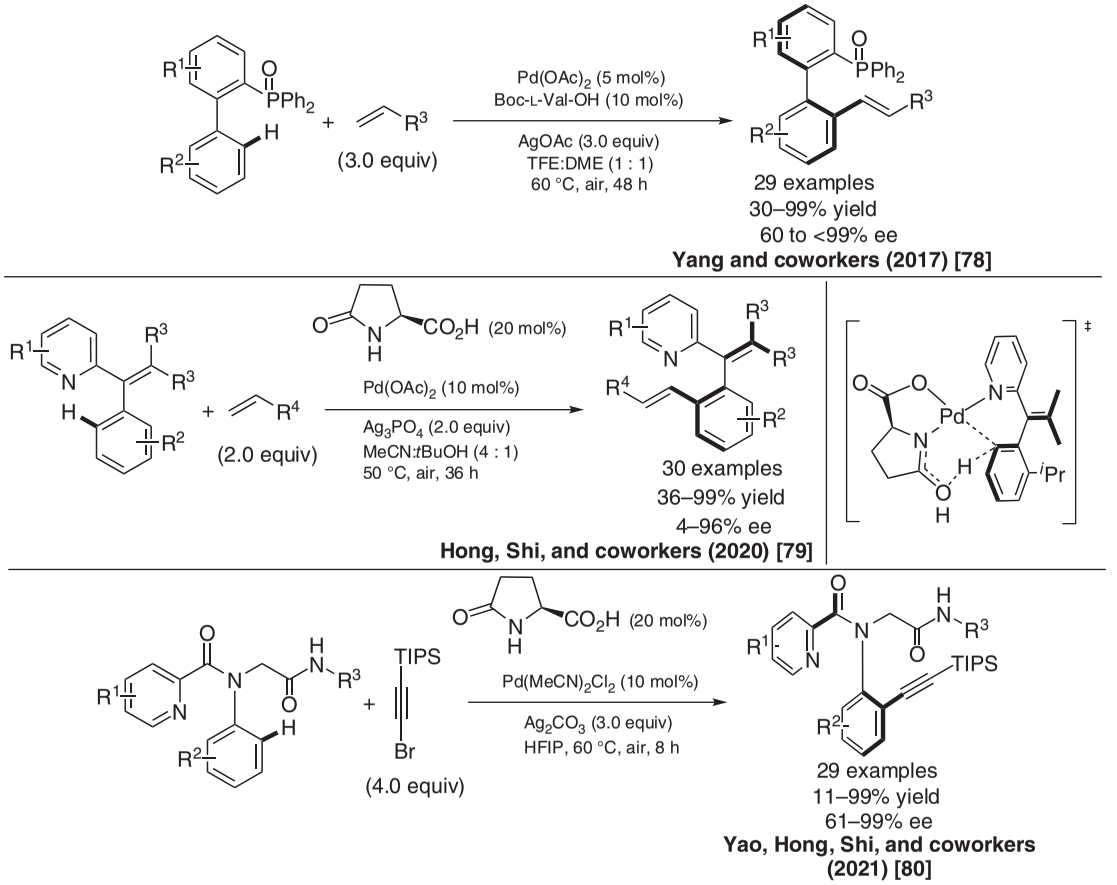

Scheme 29 Pd-catalyzed alkenylation and alkynylation to yield axially chiral compounds via atroposelective C—H activation induced by Pd complexes and amino acid ligands.

C—H activation process. In addition, the authors confirmed that racemization processes are not feasible after the C—H activation step. In 2021, Shi and coworkers also demonstrated that using the $Pd(OAc)_2$/L-pyroglutamic acid catalytic system it is possible to carry out a highly atroposelective C—H alkynylation of *N*-picolinamide peptoid anilines (Scheme 29) [80].

Other than amino acid chiral ligands, monodentate chiral phosphoric acids (CPAs), in particular those with a chiral spirocyclic core, have proven to be excellent ligands to induce enantioselectivity in these transformations, such as in a highly atroposelective C—H olefination of biaryl quinolines and unprotected anilines (Scheme 30) [81, 82].

Aldehyde-containing biaryl scaffolds can be desymmetrized using transient chiral auxiliaries (TCAs) that work as temporary directing groups. In 2017, the Shi group showed that using catalytic amounts of L-*tert*-leucine as TCA, it is possible to produce excellent levels of enantiocontrol in the desymmetrizing Pd(II)-catalyzed C—H olefination of biaryl aldehydes exhibiting free or low rotation barriers (Scheme 31) [83]. This strategy has also been successfully applied for atroposelective C—H alkynylations [84, 85] and allylations [86, 87] of biaryl aldehydes and five-membered biaryl heteroaromatic aldehydes for the naphthylation [88] and alkylation [89] of biaryl aldehydes as well as for the olefination of five-membered biaryl heteroaromatic aldehydes (Scheme 31) [90]. Remarkably, the group observed that the atroposelective C—H alkynylation of biaryl benzothiophene aldehydes gave the products with excellent enantioselectivities, whereas benzofurans failed to give enantioenriched products. DFT calculations helped to shed light into these sharp selectivity disparities by showing that the rotation barriers of the corresponding benzofuran products are generally much lower than those for benzothiophenes [85].

The same research team has also reported a method to make axially chiral styrenes from 2-arylacrylaldehydes and alkenes via asymmetric Pd(II)-catalyzed C—H olefination reactions, using an L-*tert*-leucine α-amino amide derivative as the transient chiral auxiliary (**TCA1**) (Scheme 32) [91].

3.2 Reactions Initiated by Oxidative Addition of C—X Bonds to Low-valent Transition Metals

This strategy has been rarely used for the transition metal-catalyzed enantioselective generation of atropoisomeric molecules via C—H activation processes, and the few examples published are limited to the activation of $C(sp^2)$—H bonds.

Gu and coworkers demonstrated that using $PdCl_2$/TADDOL catalytic systems it is possible to promote asymmetric intramolecular C—H arylations of indole-based atropoisomeric aryl iodides with up to 99% yield and 92% ee (Scheme 33) [92]. You and coworkers have also contributed to this approach by developing an intermolecular arylation process of quinoline-containing biaryl compounds using (hetero)aryl bromides as the coupling partners and an Rh(I)/monodentate TADDOL phosphonite as the catalytic complex (Scheme 33b) [93].

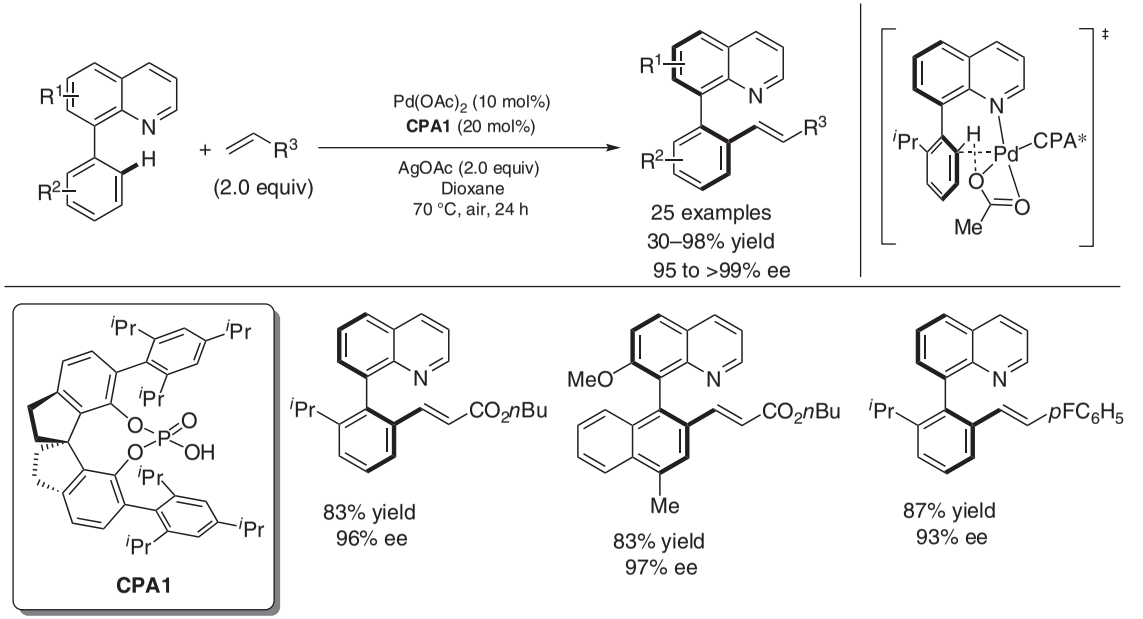

Scheme 30 Pd(II)-catalyzed alkenylation of biaryl quinolines via atroposelective C—H activation induced by chiral phosphoric acid ligands and the proposed asymmetry-inducing transition state. Source: Adapted from Li et al. [78] and Jin et al. [79].

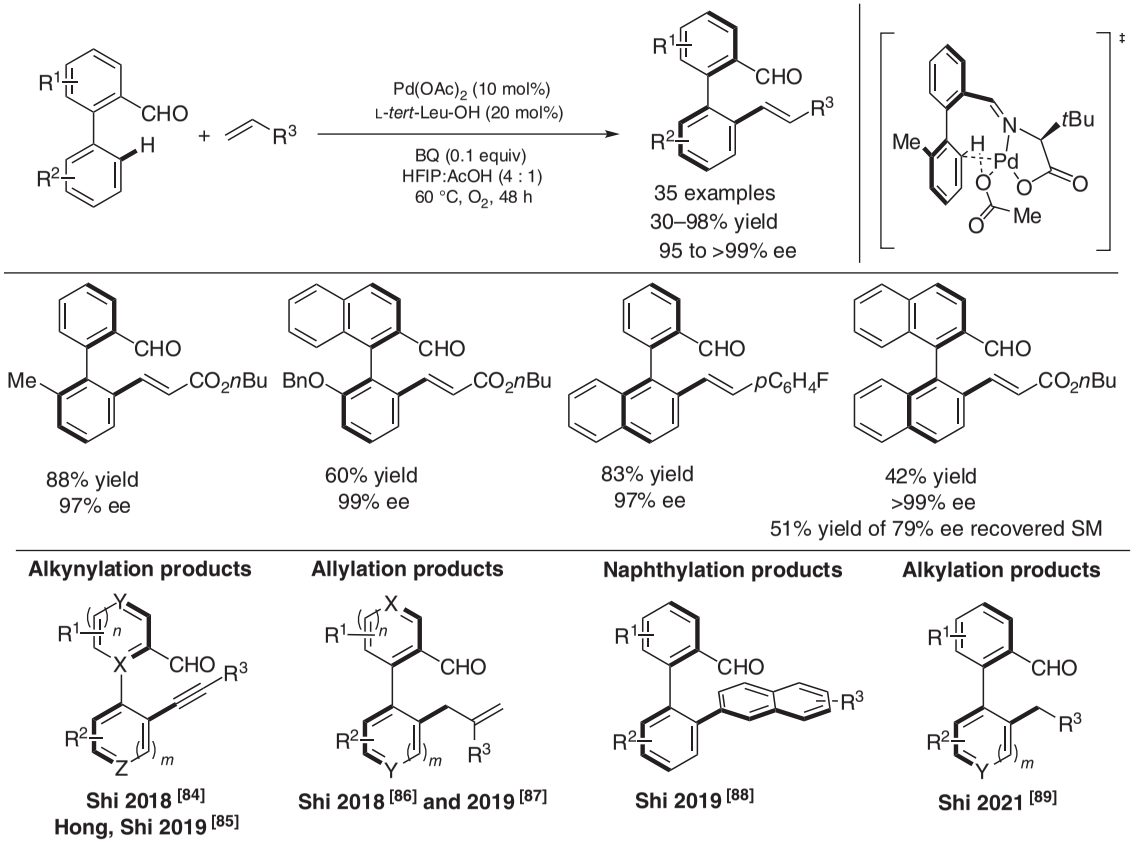

Scheme 31 Pd(II)-catalyzed atroposelective dehydrogenative Heck coupling between biaryl aldehydes and alkenes using a transient chiral auxiliary strategy.

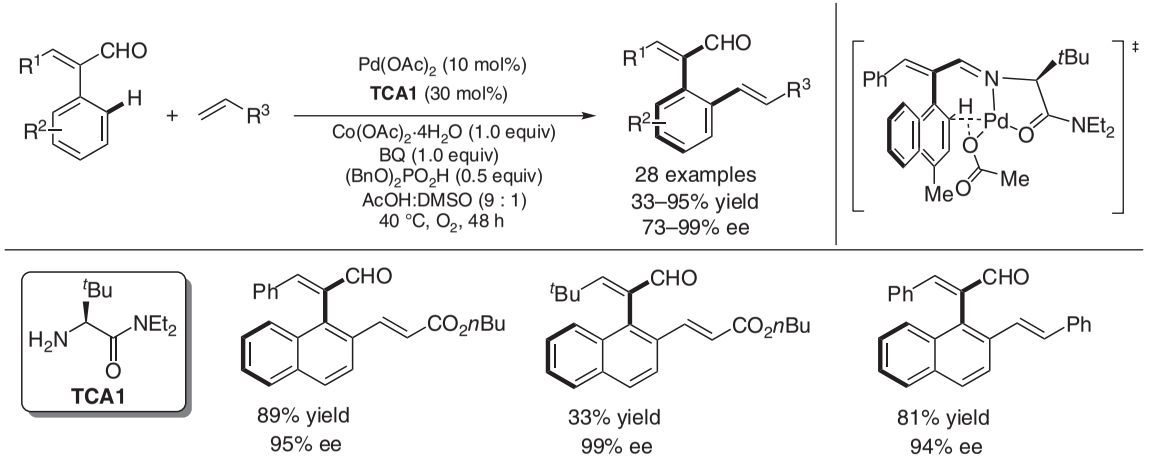

Scheme 32 Pd(II)-catalyzed atroposelective olefination between 2-arylacrylaldehydes and alkenes using a transient chiral auxiliary strategy and transition state of the atroposelective C—H activation. Source: Song et al. [91]/John Wiley & Sons.

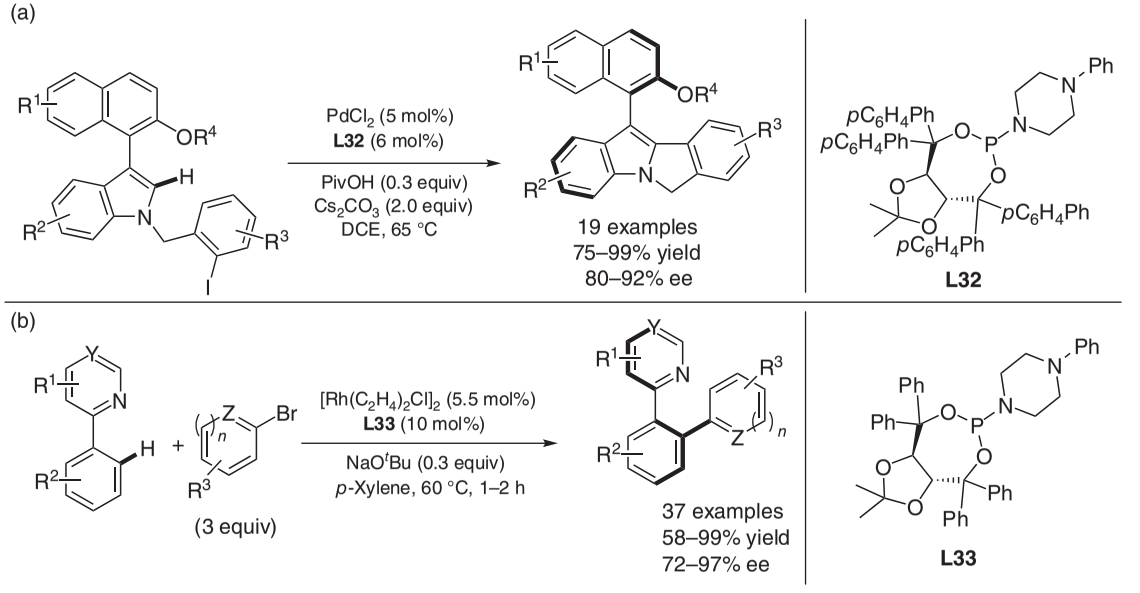

Scheme 33 Transition metal-catalyzed atroposelective transformations based on the generation of the electrophilic species after a C–halogen oxidative addition. Source: (a) He et al. [92]/American Chemical Society. (b) Wang et al. [93]/American Chemical Society.

3.3 Reactions Initiated by Oxidative Addition of C—H Bonds to Low-valent Transition Metals

There are very few examples that use this strategy to generate axial chirality.

3.3.1 C(sp^2)—H Activation

In an early example, Murai and coworkers reported the Rh(I)-catalyzed linear ethylation of 2-(1-naphthyl)-3-methylpyridine and 1-(naphthalen-1-yl)isoquinoline in modest yields and fair ees using a chiral ferrocene-based monophosphine as the ligand, and quite harsh conditions (6.8 atm of ethylene and 120 °C) [94]. More than 20 years after Murai's report, sparse examples using this approach have appeared in the literature, none of which involve enantioselective C—H activation pathways [95].

3.3.2 C(sp^3)—H Activation

Earlier this year, He and coworkers have reported a desymmetrizing atroposelective intramolecular reaction involving the activation of a benzylic methyl group [96]. The authors demonstrated that using an Rh(I) catalyst and a chiral Josiphos biphosphine ligand it is possible to promote a cyclative silylation to give six-membered biaryl silicon–stereogenic silanes with both point and axial chirality (Scheme 34). The reaction requires the use of norbornene derivatives as sacrificial hydrogen acceptors.

4 Desymmetrizations Generating Planar Chirality

The last section of this review deals with desymmetrizing reactions that generate planar chirality in metallocene or metal arene complexes, a topic that has also been yet scarcely explored. After an initial example in 2013, most of the methodologies so far reported describe the synthesis of planar chiral ferrocenes [97–99], although some recent reports dealing with the synthesis of planar chiral ruthenocenes and arene chromium complexes, have been published [97, 98].

4.1 Reactions Catalyzed by Electrophilic Transition Metal Complexes

One of the earliest examples of desymmetrizing C—H functionalizations generating planar chirality is the Pd(II)-catalyzed dehydrogenative Heck-type alkenylation of dialkylaminomethylferrocenes with olefins, including challenging alkyl olefins, using MPAA (in this case Boc-L-Val-OH) as the chirality-inducing ligand (Scheme 35a) [100]. Other transformations of aminomethyl ferrocene that also operate via Pd(II)/Pd(0) redox cycles, including arylations with arylboronic acids [101] and annulations [102] with diarylethynes, have also been described (Scheme 35b). This last transformation generates enantioenriched naphthyl-substituted ferrocene derivatives after the incorporation of two molecules of the alkyne into the ferrocenyl moiety. An asymmetric oxidative Pd(II)-catalyzed coupling between dimethylaminomethyl ferrocene derivatives and heteroarenes was published in 2016 by the

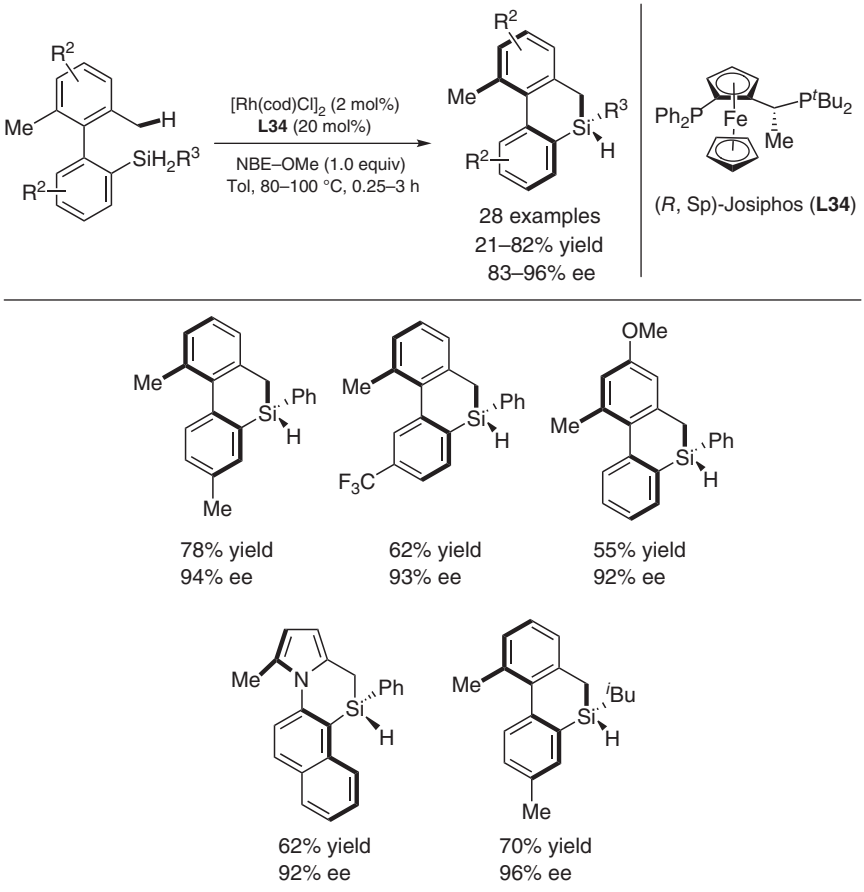

Scheme 34 Rh(I)-catalyzed atroposelective intramolecular silylation of biaryl dihydrosilanes via C(sp^3)—H activation. NBE–OMe = 5-(methoxymethyl)bicyclo[2.2.1] hept-2-ene.

You group. This work described a biaryl coupling reaction occurring via twofold C—H activation using MPAA ligands, air as the oxidant, and benzofuran, benzothiophene, indole, furan, thiophene, or pyrroles as coupling partners (Scheme 35b) [103]. This method was subsequently extended to the coupling of azoles using very similar reaction conditions (Scheme 35b) [104]. MPAAs have also been used in combination with strong oxidants to carry out transformations entailing Pd(II)/Pd(IV) redox cycles. *tert*-Butyl hydroperoxide (TBHP) has been used as the oxidant in the C—H acylation of dimethylaminomethylferrocene derivatives using symmetrical diketones as ketone source (Scheme 35b) [105].

The use of MPAAs as chiral ligands has also been extended to substrates other than dialkylaminomethylferrocenes. For instance, Ac-L-Phe-OH has proven an effective ligand for the Pd(II)-catalyzed alkenylation of the ferrocenecarboxylic acid, although leading to moderate enantiomeric excesses [106].

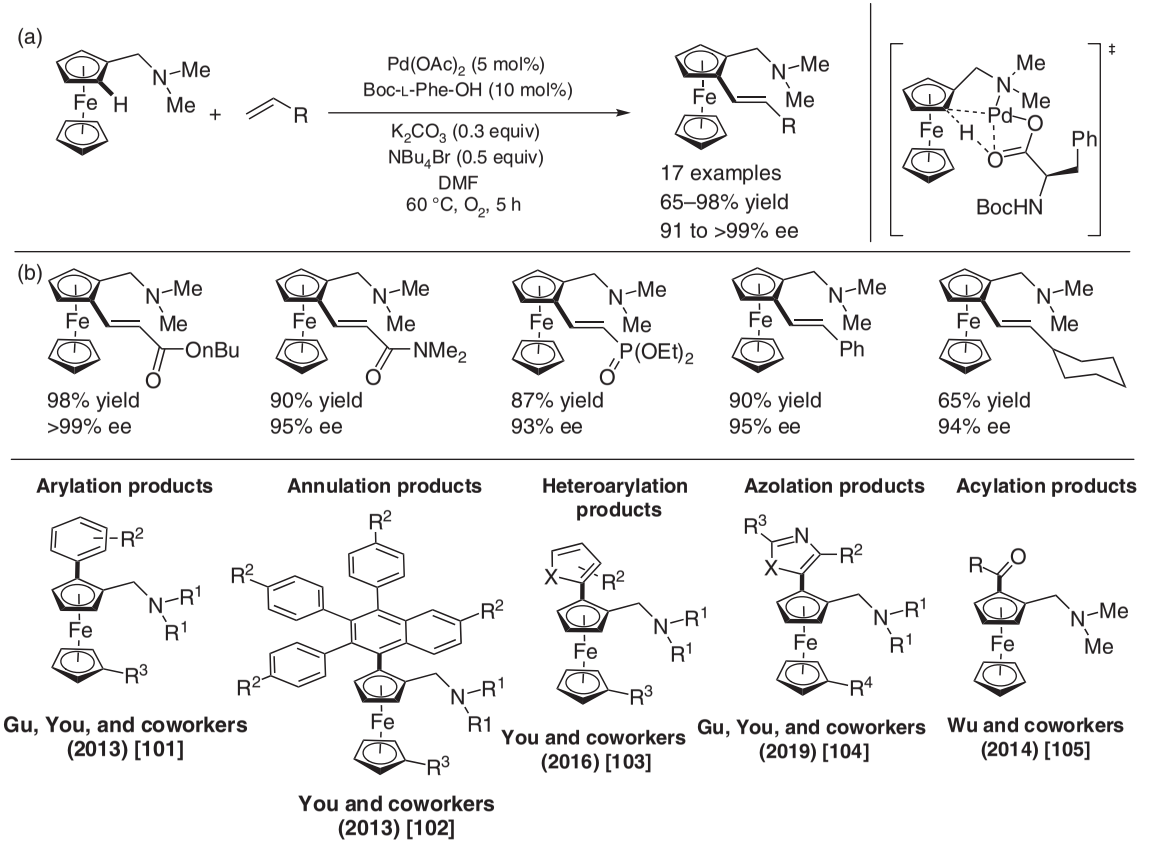

Scheme 35 Pd(II)-catalyzed dehydrogenative oxidative coupling between dimethylaminomethylferrocene and alkenes with Boc-L-Phe-OH as the chiral ligand. Other Pd(II)-catalyzed enantioselective C—H functionalizations of dialkylamino methylferrocene using MPAA ligands. Source: (a) Pi et al. [100]/Royal Society of Chemistry.

Similar to MPAAs, unprotected α-amino acids, such as L-*tert*-leucine, have been used as transient chiral mediators in the desymmetrizing arylation of ferrocenyl ketones using aryl and heteroaryl iodides as coupling partners (Scheme 36) [107].

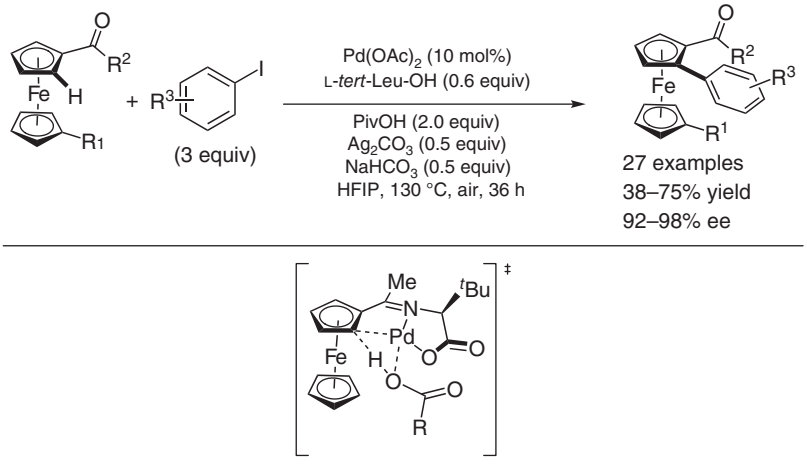

Scheme 36 Pd(II)-catalyzed C—H arylations of ferrocenyl ketones with aryl iodides and L-*tert*-leucine as the chiral transient mediator. Source: Xu et al. [107]/Royal Society of Chemistry.

Other than palladium-based catalysts, a scandium(III) half-sandwich complex bearing a chiral C_2-symmetrical Cp ligand was found a competent catalyst for the highly enantioselective C—H alkenylation of quinoline- and pyridine-substituted ferrocenes with internal alkynes [108]. Moreover, achiral CpM(III) complexes of group 9 transition metals in combination with a chiral MPAA or a CCA ligand have been shown to effectively catalyze the atroposelective C—H amidation of ferrocenes bearing a directing group. In particular, in 2019, the Shi group reported the amidation of thiomide-containing ferrocenes with Cp*Co catalysts using benzyl-protected D-*p*-hydroxylphenylglycine ligands, although in modest enantioselectivities. They also extended these transformations to amide-containing ferrocenes using a modified Cp*Ir catalyst with a CCA (Scheme 37) [109, 110].

In 2019, the Larrosa group published a method for the desymmetrizing C—H arylation of (η^6-arene)chromium complexes by synergistic silver and palladium catalysis using an hemilabile H_8–BINAP(O) chiral ligand (Scheme 38) [111]. The authors postulated an enantiodetermining C—H activation of the arenechromium complexes by silver carboxylates to generate a chiral arylsilver complex that transmetalates to Pd as a plausible mechanistic pathway.

4.2 Reactions Initiated by Oxidative Additions of C—X Bonds to Low-valent Transition Metals

Axially chiral ferrocene and ruthenocene derivatives have also been obtained via electrophilic C(sp^2)—Pd^{II} species generated by oxidative addition across

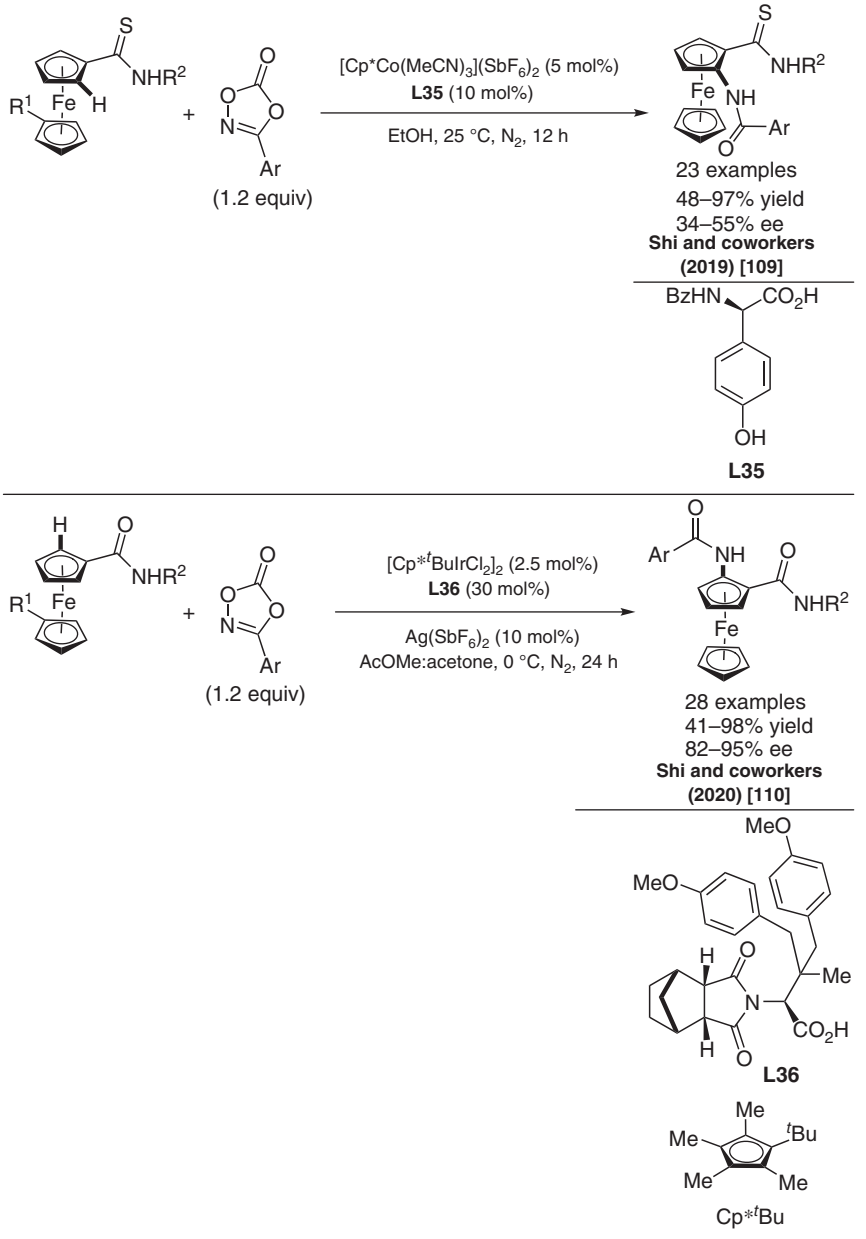

Scheme 37 CpM-catalyzed C—H amidations of ferrocene derivatives with diazolones using MPAAs or CCAs as chiral inducers.

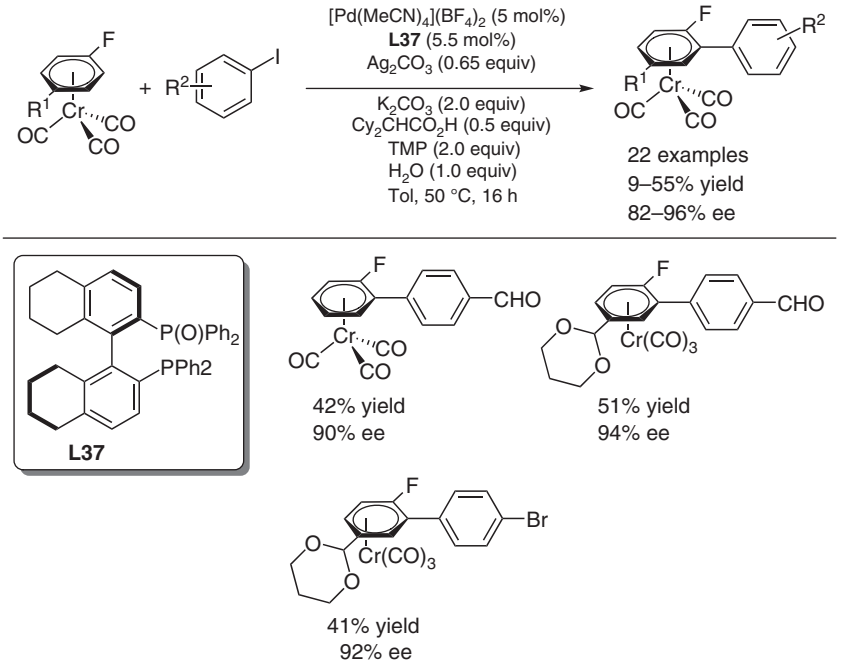

Scheme 38 Ag(I)-mediated/Pd(0)-catalyzed desymmetric C—H arylations of (η^6-arene)chromium complexes using aryl iodides and H_8–BINAP(O) as the chiral ligand. Source: Batuecas et al. [111]/American Chemical Society.

C(sp^2)–halogen bonds in aryl or alkenyl moieties appended to the ferrocene moieties. In 2014, Kang, Gu, and coworkers and You and coworkers independently reported the desymmetrizing arylative cyclization of *o*-halobenzoylferrocene derivatives [112–114]. Using chiral BINAP ligands, Kang and Gu's method afforded chiral indanone-fused ferrocene and ruthenocene products from aryl iodides (Scheme 39), whereas You's method yielded chiral ferrocenes from aryl bromides, also using BINAP ligands under very similar reaction conditions.

The You group further expanded the cyclizations to the C(sp^2)—H heteroarylation and alkenylation of ferrocenyl derivatives (Scheme 39) [115, 116]. These methodologies delivered chiral indanone-fused ferrocenylpyridine and ferrocenylcyclohexene products from their parent pyridyl bromide or chloride and cyclohexyl bromide precursors.

Related processes involving desymmetrizing palladium-catalyzed arylative cyclization of *N*-(2-haloaryl)-ferrocenecarboxamides have been used to produce quinolinone-fused ferrocene derivatives, using chiral TADDOL-derived phosphoramidites or 1-[2-(diphenylphosphino)-1-naphthalenyl]-4-[1-phenylethoxy]phthalazine (O–PINAP) as the enantioinducing ligands (Scheme 39) [117, 118].

Other than carbonyl ferrocenyl derivatives, *o*-bromophenyl ferrocenyl sulfides have been reported to undergo enantioselective Pd-catalyzed cyclative arylations in the presence of Segphos to afford planar chiral benzothiophene-fused ferrocenes (Scheme 39) [119].

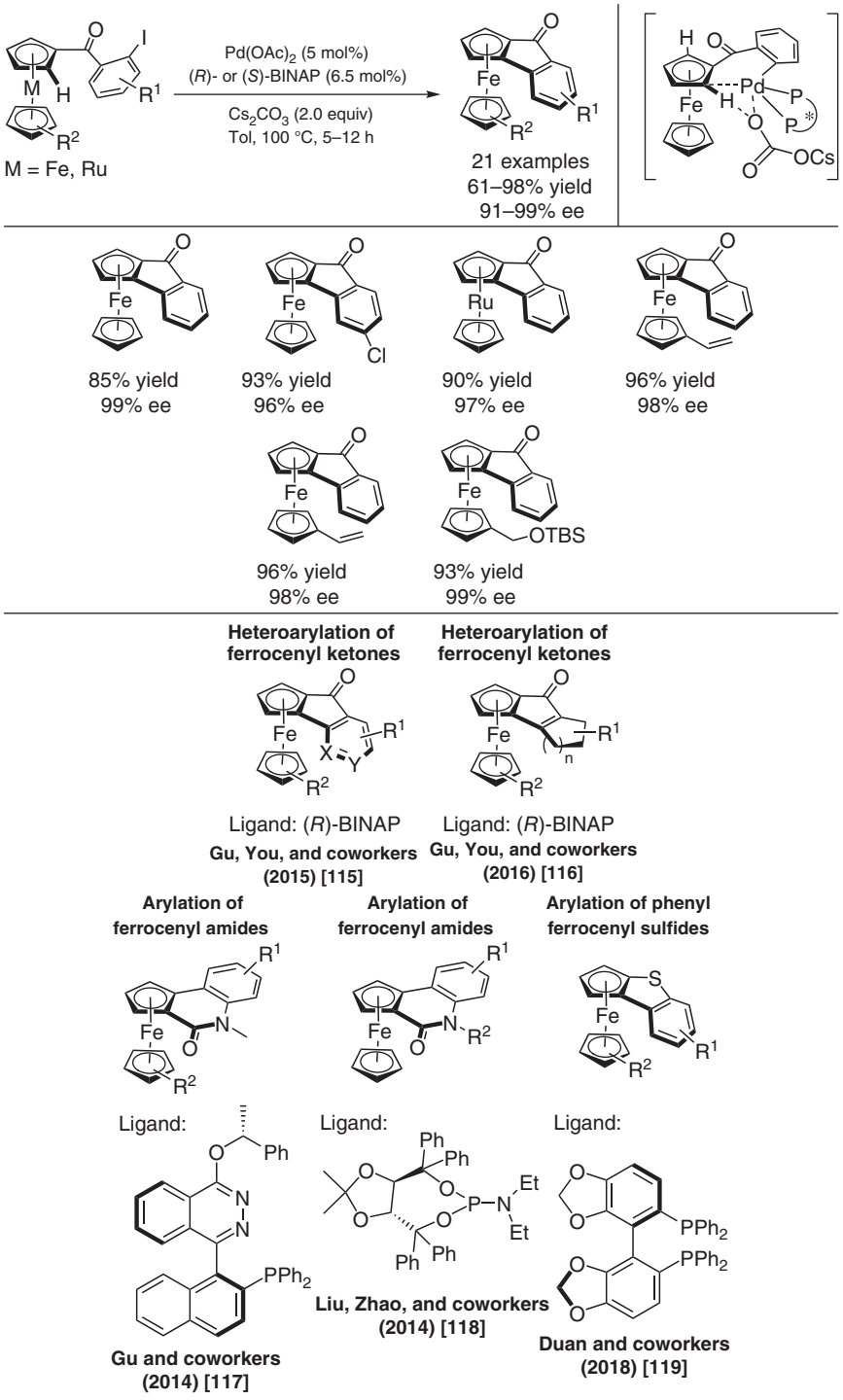

Scheme 39 Pd(0)-catalyzed intramolecular C—H arylations and alkenylation of ferrocenyl ketones and amides.

Intermolecular reactions based on these types of C—H activation sequences have also been reported. The You group has recently described examples of enantioselective arylation of ferrocenyl thioketones and pyridylferrocenes using aryl iodides or bromides as the coupling partners and Rh(I)/TADDOL-based phosphonites as catalytic systems [120, 121]. In related intermolecular processes, Luo, Zhu, and coworkers applied imidoylation protocols previously used to generate point chirality [36] (see Section 2.2.1) to the synthesis of planar chiral ferrocenes. The authors explored this concept to develop a method for the synthesis of enantioenriched pyridoferrocenes from ferrocenyl isocyanide derivatives and aryl iodides or bromides by Pd-catalyzed domino isocyanide insertion/enantioselective C—H cyclization processes (Scheme 40) [122]. In a similar approach, Liu and coworkers developed a protocol for the preparation of planar chiral ferrocene[1,2-*d*] pyrrolidones via Pd-catalyzed alkyne insertion/enantioselective C—H cyclization of ferrocenyl scaffolds bearing internal alkyne pendants (Scheme 40) [123].

4.3 Reactions Initiated by Oxidative Addition of C—H Bonds at Low-valent Transition Metals

This C—H activation strategy, which in general is based on the use of low-valent group 9 transition metals, has also been used for the enantioselective transformation of precursors with planar symmetry. In 2014, Shibata and Shizuno reported the use of a catalytic system made of $[\{Ir(I)(coe)_2Cl\}_2]$ and a chiral diene ligand to promote the enantioselective monoalkylation of quinoline-containing ferrocene derivatives using alkenes as the coupling partners (Scheme 41) [124].

He and coworkers, and the groups of Murai and Takai, independently developed an efficient Rh(I)-catalyzed desymmetrizing silacyclization of benzosilylometallocenes derivatives using axially chiral diphosphine ligands [125, 126]. The He group demonstrated that using (*S*)-TMS–SEGPHOS as chiral ligand, this dehydrogenative process can be applied to a wide range of ferrocene and ruthenocene derivatives with good yields and enantioselectivities (Scheme 41a) [126]. A related Rh(I)-catalyzed enantioselective direct cyclative silylation was reported by Shibata et al. using chiral diene ligands. This transformation requires the use of a sacrificial alkene as a hydrogen acceptor in order to increase the reaction yields and enantioselectivities (Scheme 41b) [127]. Importantly, the reaction could be extended to the dehydrogenative coupling of the (dimethylhydrogermyl)phenylferrocene derivatives, although in lower yields and enantioselectivities. Zhao et al. described in 2018 a two-step strategy for the assembly of planar chiral ferrocene oxasilolanes via Ir-catalyzed silylation of ferrocenyl phenols followed by asymmetric Rh(I)-catalyzed intramolecular C—H silylation of benzosilylometallocenes using chiral Josiphos ligand **L42** (Scheme 41c) [128].

Finally, Ye and coworkers used a different strategy based on Ni catalysis to obtain highly enantioenriched planar chiral ferrocene derivatives. The authors described an Ni^0-catalyzed enantioselective formal cycloaddition between ferrocenyl formamide compounds and alkynes (Scheme 42) [129]. This strategy made use

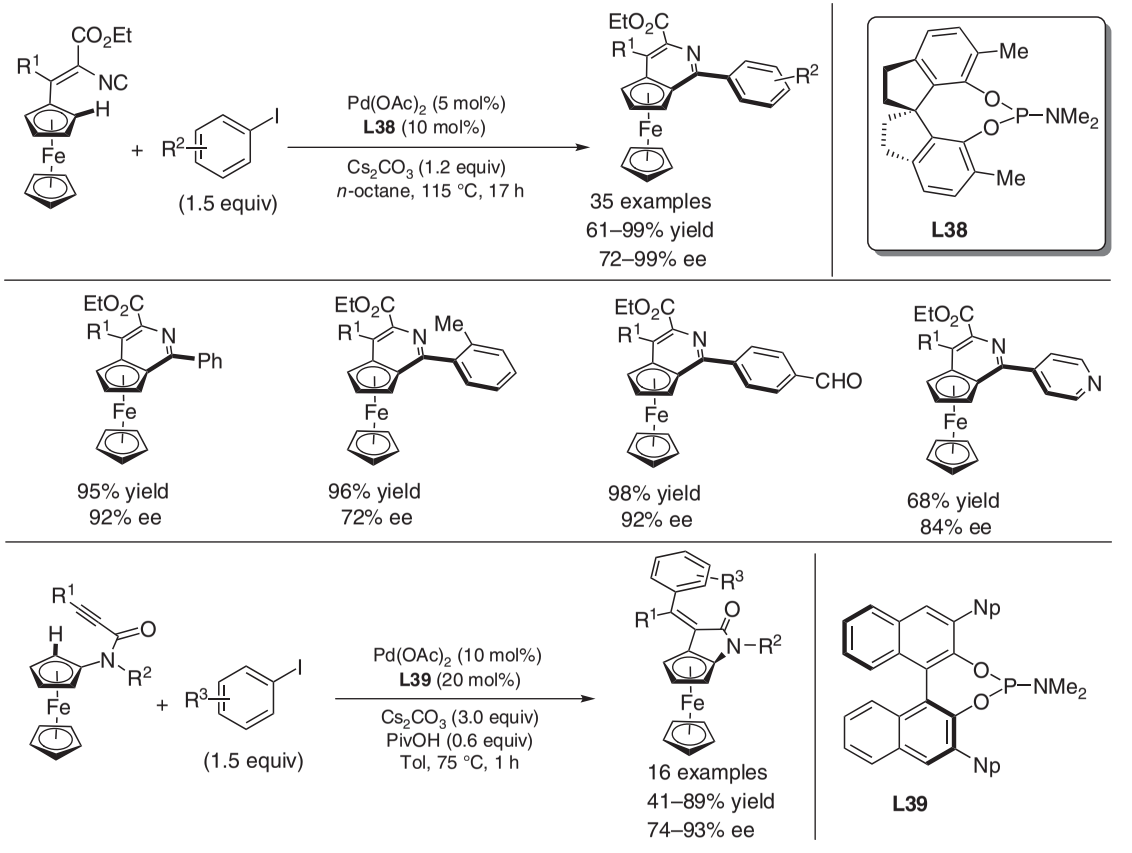

Scheme 40 Pd(0)-catalyzed desymmetric hydroarylation/C—H cyclizations of ferrocenyl derivatives. Source: Adapted from Luo et al. [122] and Jia et al. [123].

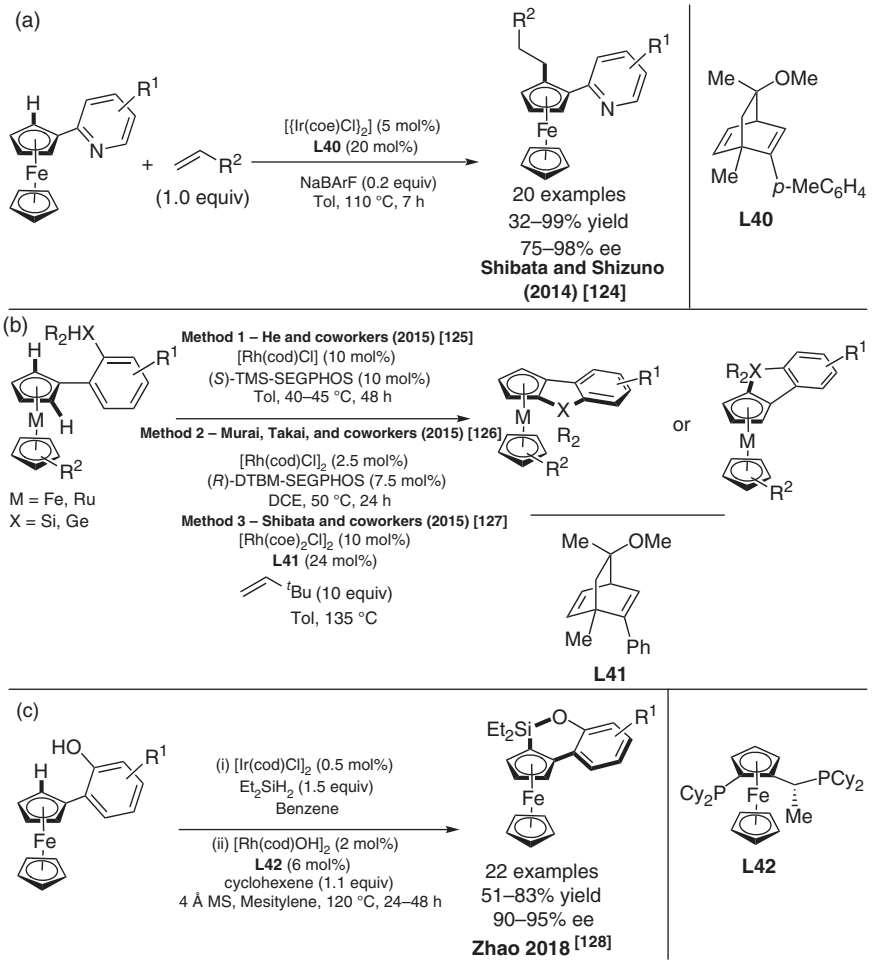

Scheme 41 Low-valent group IX-catalyzed desymmetric C—H functionalization of ferrocenyl derivatives to obtain planar chiral products.

of the ability of Ni^0 catalysts to promote the C—H oxidative addition of Lewis acid-activated formamides. Once the acyl–Ni^{II} intermediate forms upon C—H oxidative addition, subsequent desymmetrizing C—H activation takes place, followed by the migratory insertion of the alkyne. A final C—C reductive elimination provides the annulated product.

5 Conclusions and Outlook

This article reviews the progress in the field of metal-catalyzed desymmetrizing functionalizations of C—H bonds in reactions involving enantiodetermining C—H activation steps. This field is still young, but it is increasingly flourishing. The structural simplicity of the precursors owing to their intrinsic symmetry, the possibility of using different C—H activation mechanisms, and the variety of metals

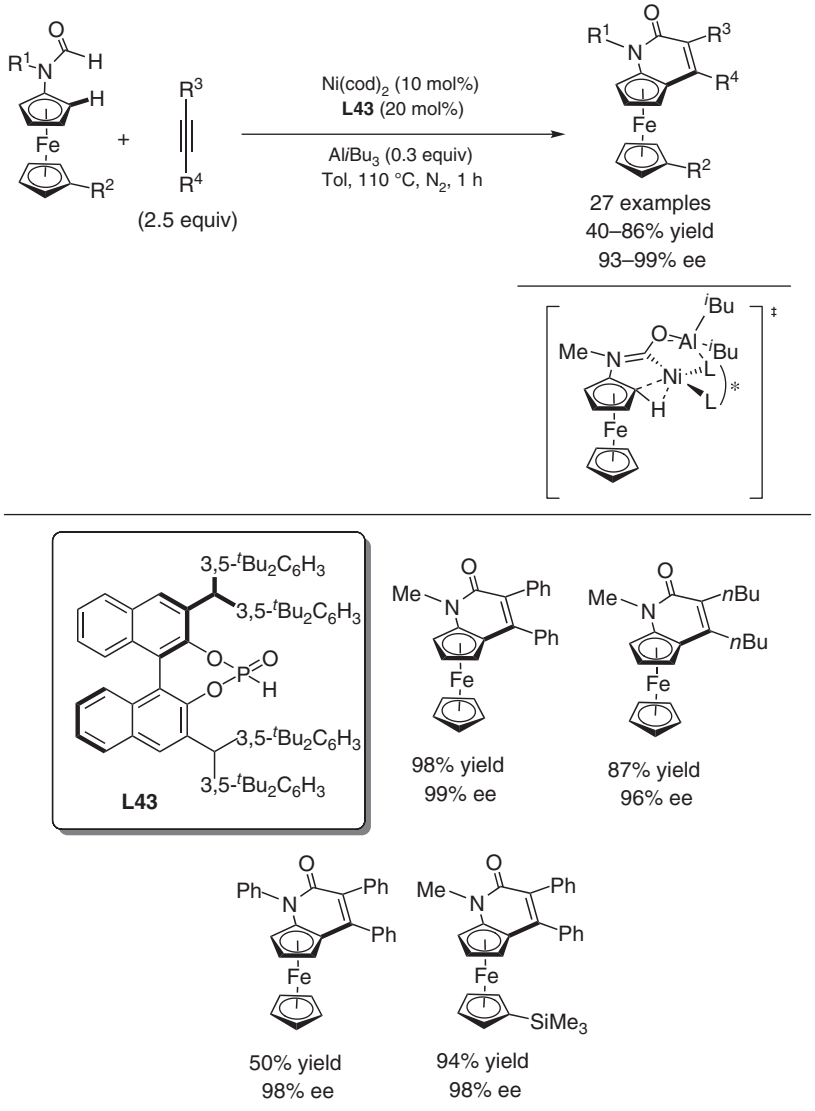

Scheme 42 Ni(0)-catalyzed formal (4 + 2) cycloaddition between ferrocenyl formamides and alkynes to yield planar chiral pyridone-fused ferrocenyl compounds and proposed transition state for the C—H activation step. Source: Chen et al. [129]/John Wiley & Sons.

and chiral ligands that can be used, place these methods among the more powerful tools in the field of asymmetric catalysis.

However, many important challenges remain. In an important number of protocols, the efficiency and stereoselectivity of the desymmetrizing reactions needs to be further improved, and their scope broadened. Thus, a new generation of catalysts with improved efficiency and selectivity and broader applicability is required. Toward this end, computational studies of catalyst/substrate interactions

can be an invaluable tool to better tailor and predict effective ligands. Moreover, expanding the approaches to activate a broader variety of C(sp^3)—H bonds and increasing the number of metals than can be used, especially 3d metals, which are less expensive and more sustainable than Pd, Rh, or Ir, are relevant challenges for the near future.

Acknowledgments

This work has received financial support from Spanish grants (PID2019-108624RB-I00, PID2019-110385GB-I00, FPU fellowship to Xandro Vidal, and JdC-I fellowship to Marc Font), the Consellería de Cultura, Educación e Ordenación Universitaria (ED431C-2021/25, 2021-CP054 and Centro Singular de Investigación de Galicia accreditation 2019–2022, ED431G 2019/03), and the European Regional Development Fund (ERDF).

Related Articles

Natural Product Synthesis via Pd-Catalyzed C—H Activation
Palladium-Catalyzed Asymmetric C(sp^2)—H Functionalization
Asymmetric Addition of Inert C—H Bond to Carbonyls, Imines, and Electron-Deficient Alkenes
Rhodium-Catalyzed Enantioselective C—H Functionalization Using Chiral Cp Ligands
Late-Stage C—H Functionalization of Natural Products, Drugs, Clinical Trial Agents, and Biomolecules: In View of Molecular Property and Mechanistic Pathway
Catalytic Enantioselective C—H Borylation
Cobalt-Catalyzed Asymmetric C—H Functionalization
Iridium-Catalyzed Asymmetric C—H Functionalization
Ruthenium-Catalyzed Asymmetric C—H Functionalization
Nickel-Catalyzed Asymmetric C—H Functionalization
Asymmetric C—H Functionalization of Ferrocene
Transition Metal-Catalyzed Atropisomer Synthesis via C—H Functionalization
Chiral Cyclopentadienyl Ligand for Asymmetric C—H Activation
Transition Metal-Catalyzed Stereo- and Chemoselective Alkenyl C—H Functionalizations
C—H Functionalization-Based Strategy in the Synthesis of Drug Molecules

References

1 Newton, C.G., Wang, S.-G., Oliveira, C.C. et al. (2017). *Chem. Rev.* 117: 8908–8976.
2 Achar, T.K., Maiti, S., Jana, S. et al. (2020). *ACS Catal.* 10: 13748–13793.

3 Saint-Denis, T.G., Zhu, R.Y., Chen, G. et al. (2018). *Science* 80 (359): 1–12.
4 González, J.M., Cendón, B., Mascareñas, J.L. et al. (2021). *J. Am. Chem. Soc.* 143: 3747–3752.
5 Engle, K.M. (2016). *Pure Appl. Chem.* 88: 119–138.
6 Shao, Q., Wu, K., Zhuang, Z. et al. (2020). *Acc. Chem. Res.* 53: 833–851.
7 Shi, B.F., Maugel, N., Zhang, Y.H. et al. (2008). *Angew. Chem. Int. Ed.* 47: 4882–4886.
8 Shi, B.F., Zhang, Y.H., Lam, J.K. et al. (2010). *J. Am. Chem. Soc.* 132: 460–461.
9 Du, Z.J., Guan, J., Wu, G.J. et al. (2015). *J. Am. Chem. Soc.* 137: 632–635.
10 Laforteza, B.N., Chan, K.S.L., and Yu, J.Q. (2015). *Angew. Chem. Int. Ed.* 54: 11143–11146.
11 Zhu, Y.C., Li, Y., Zhang, B.C. et al. (2018). *Angew. Chem. Int. Ed.* 57: 5129–5133.
12 Vidal, X., Mascareñas, J.L., and Gulías, M. (2019). *J. Am. Chem. Soc.* 141: 1862–1866.
13 Bai, X.F., Mu, Q.C., Xu, Z. et al. (2019). *ACS Catal.* 9: 1431–1436.
14 Han, H., Zhang, T., Yang, S.D. et al. (2019). *Org. Lett.* 21: 1749–1754.
15 Cheng, X.F., Li, Y., Su, Y.M. et al. (2013). *J. Am. Chem. Soc.* 135: 1236–1239.
16 Chu, L., Wang, X.C., Moore, C.E. et al. (2013). *J. Am. Chem. Soc.* 135: 16344–16347.
17 Lin, L., Fukagawa, S., Sekine, D. et al. (2018). *Angew. Chem. Int. Ed.* 57: 12048–12052.
18 Sun, Y. and Cramer, N. (2018). *Angew. Chem. Int. Ed.* 57: 15539–15543.
19 Shen, B., Wan, B., and Li, X. (2018). *Angew. Chem. Int. Ed.* 57: 15534–15538.
20 Li, X., Hu, P., Kong, L. et al. (2021). *Angew. Chem. Int. Ed.* doi: 10.1002/anie.202106871.
21 Jang, Y.S., Dieckmann, M., and Cramer, N. (2017). *Angew. Chem. Int. Ed.* 56: 15088–15092.
22 Jang, Y.S., Woźniak, Ł., Pedroni, J. et al. (2018). *Angew. Chem. Int. Ed.* 57: 12901–12905.
23 Xiao, K.J., Lin, D.W., Miura, M. et al. (2014). *J. Am. Chem. Soc.* 136: 8138–8142.
24 He, J., Shao, Q., Wu, Q. et al. (2017). *J. Am. Chem. Soc.* 139: 3344–3347.
25 Hu, L., Shen, P.X., Shao, Q. et al. (2019). *Angew. Chem. Int. Ed.* 58: 2134–2138.
26 Wasa, M., Engle, K.M., Lin, D.W. et al. (2011). *J. Am. Chem. Soc.* 133: 19598–19601.
27 Wu, Q.F., Shen, P.X., He, J. et al. (2017). *Science* 80 (355): 499–503.
28 Zhuang, Z. and Yu, J.Q. (2020). *Nature* 577: 656–659.
29 Chan, K.S.L., Fu, H.Y., and Yu, J.Q. (2015). *J. Am. Chem. Soc.* 137: 2042–2046.
30 Shen, P.X., Hu, L., Shao, Q. et al. (2018). *J. Am. Chem. Soc.* 140: 6545–6549.
31 Smalley, A.P., Cuthbertson, J.D., and Gaunt, M.J. (2017). *J. Am. Chem. Soc.* 139: 1412–1415.
32 Liu, B., Xie, P., Zhao, J. et al. (2021). *Angew. Chem. Int. Ed.* 60: 8396–8400.
33 Kato, Y., Lin, L., Kojima, M. et al. (2021). *ACS Catal.* 11: 4271–4277.
34 Albicker, M.R. and Cramer, N. (2009). *Angew. Chem. Int. Ed.* 48: 9139–9142.
35 Saget, T. and Cramer, N. (2013). *Angew. Chem. Int. Ed.* 52: 7865–7868.
36 Wang, J., Gao, D.-W., Huang, J. et al. (2017). *ACS Catal.* 7: 3832–3836.

37 Lin, Z.Q., Wang, W.Z., Yan, S.B. et al. (2015). *Angew. Chem. Int. Ed.* 54: 6265–6269.
38 Liu, L., Zhang, A.A., Wang, Y. et al. (2015). *Org. Lett.* 17: 2046–2049.
39 Xu, G., Li, M., Wang, S. et al. (2015). *Org. Chem. Front.* 2: 1342–1345.
40 Grosheva, D. and Cramer, N. (2017). *ACS Catal.* 7: 7417–7420.
41 Shintani, R., Otomo, H., Ota, K. et al. (2012). *J. Am. Chem. Soc.* 134: 7305–7308.
42 Lin, Y., Ma, W.Y., Sun, Q.Y. et al. (2017). *Synlett* 28: 1432–1436.
43 Li, Z., Lin, Z.Q., Yan, C.G. et al. (2019). *Organometallics* 38: 3916–3920.
44 Yang, L., Neuburger, M., and Baudoin, O. (2018). *Angew. Chem. Int. Ed.* 57: 1394–1398.
45 Anas, S., Cordi, A., and Kagan, H.B. (2011). *Chem. Commun.* 47: 11483–11485.
46 Yang, L., Melot, R., Neuburger, M. et al. (2017). *Chem. Sci.* 8: 1344–1349.
47 Melot, R., Craveiro, M.V., Bürgi, T. et al. (2019). *Org. Lett.* 21: 812–815.
48 Kong, W.X., Xie, S.J., Cao, C.Y.Z. et al. (2020). *Chem. Commun.* 56: 2292–2295.
49 Nakanishi, M., Katayev, D., Besnard, C. et al. (2011). *Angew. Chem. Int. Ed.* 50: 7438–7441.
50 Saget, T., Lemouzy, S.J., and Cramer, N. (2012). *Angew. Chem. Int. Ed.* 51: 2238–2242.
51 Martin, N., Pierre, C., Davi, M. et al. (2012). *Chem. A Eur. J.* 18: 4480–4484.
52 Holstein, P.M., Vogler, M., Larini, P. et al. (2015). *ACS Catal.* 5: 4300–4308.
53 Larionov, E., Nakanishi, M., Katayev, D. et al. (2013). *Chem. Sci.* 4: 1995–2005.
54 Saget, T. and Cramer, N. (2012). *Angew. Chem. Int. Ed.* 51: 12842–12845.
55 Pedroni, J., Saget, T., Donets, P.A. et al. (2015). *Chem. Sci.* 6: 5164–5171.
56 Pedroni, J. and Cramer, N. (2015). *Angew. Chem. Int. Ed.* 54: 11826–11829.
57 Ladd, C.L. and Charette, A.B. (2016). *Org. Lett.* 18: 6046–6049.
58 Mayer, C., Ladd, C.L., and Charette, A.B. (2019). *Org. Lett.* 21: 2639–2644.
59 Fernández, D.F., Mascareñas, J.L., and López, F. (2020). *Chem. Soc. Rev.* 49: 7378–7405.
60 Kuninobu, Y., Yamauchi, K., Tamura, N. et al. (2013). *Angew. Chem. Int. Ed.* 52: 1520–1522.
61 Lee, T., Wilson, T.W., Berg, R. et al. (2015). *J. Am. Chem. Soc.* 137: 6742–6745.
62 Su, B., Zhou, T.G., Li, X.W. et al. (2017). *Angew. Chem. Int. Ed.* 56: 1092–1096.
63 Su, B., Zhou, T.G., Xu, P.L. et al. (2017). *Angew. Chem. Int. Ed.* 56: 7205–7208.
64 Zou, X., Zhao, H., Li, Y. et al. (2019). *J. Am. Chem. Soc.* 141: 5334–5342.
65 Genov, G.R., Douthwaite, J.L., Lahdenperä, A.S.K. et al. (2020). *Science* 80 (367): 1246–1251.
66 Murai, M., Takeshima, H., Morita, H. et al. (2015). *J. Organomet. Chem.* 80: 5407–5414.
67 Su, B. and Hartwig, J.F. (2017). *J. Am. Chem. Soc.* 139: 12137–12140.
68 Lee, T. and Hartwig, J.F. (2016). *Angew. Chem. Int. Ed.* 55: 8723–8727.
69 Carmona, J.A., Rodríguez-Franco, C., Fernández, R. et al. (2021). *Chem. Soc. Rev.* 50: 2968–2983.
70 Liu, C.-X., Zhang, W.-W., Yin, S.-Y. et al. (2021). *J. Am. Chem. Soc.* doi: 10.1021/jacs.1c07635.
71 Ye, B. and Cramer, N. (2013). *J. Am. Chem. Soc.* 135: 636–639.

72 Zheng, J. and You, S.-L. (2014). *Angew. Chem. Int. Ed.* 53: 13244–13247.
73 Mas-Roselló, J., Herraiz, A., Audic, B. et al. (2020). *Angew. Chem. Int. Ed.* 60: 13198–13244.
74 Sun, L., Chen, H., Liu, B. et al. (2021). *Angew. Chem. Int. Ed.* 60: 8391–8395.
75 Zheng, J., Cui, W.-J., Zheng, C. et al. (2016). *J. Am. Chem. Soc.* 138: 5242–5245.
76 Wang, Q., Zhang, W.-W., Song, H. et al. (2020). *J. Am. Chem. Soc.* 142: 15678–15685.
77 Wang, Q., Zhang, W.-W., Zheng, C. et al. (2021). *J. Am. Chem. Soc.* 143: 114–120.
78 Li, S.-X., Ma, Y.-N., and Yang, S.D. (2017). *Org. Lett.* 19: 1842–1845.
79 Jin, L., Yao, Q.-J., Xie, P.-P. et al. (2020). *Chem* 6: 497–511.
80 Wu, Y.-J., Xie, P.-P., Zhou, G. et al. (2021). *Chem. Sci.* doi: 10.1039/d1sc01130h.
81 Luo, J., Zhang, T., Wang, L. et al. (2019). *Angew. Chem. Int. Ed.* 58: 6708–6712.
82 Zhan, B.-B., Wang, L., Luo, J. et al. (2020). *Angew. Chem. Int. Ed.* 59: 3568–3572.
83 Yao, Q.-J., Zhang, S., Zhan, B.-B. et al. (2017). *Angew. Chem. Int. Ed.* 56: 6617–6621.
84 Liao, G., Yao, Q.-J., Zhang, Z.-Z. et al. (2018). *Angew. Chem. Int. Ed.* 57: 3661–3665.
85 Zhang, S., Yao, Q.-J., Liao, G. et al. (2019). *ACS Catal.* 9: 1956–1961.
86 Liao, G., Li, B., Chen, H.-M. et al. (2018). *Angew. Chem. Int. Ed.* 57: 17151–17155.
87 Chen, H.-M., Zhang, S., Liao, G. et al. (2019). *Organometallics* 38: 4022–4028.
88 Liao, G., Chen, H.-M., Xia, Y.-N. et al. (2019). *Angew. Chem. Int. Ed.* 58: 11464–11468.
89 Chen, H.-M., Liao, G., Xu, C.-K. et al. (2021). *CCS Chem.* 3: 455–465.
90 Zhang, J., Xu, Q., Wu, J. et al. (2019). *Org. Lett.* 21: 6361–6365.
91 Song, H., Li, Y., Yao, Q.J. et al. (2020). *Angew. Chem. Int. Ed.* 59: 6576–6580.
92 He, C., Hou, M., Zhu, Z. et al. (2017). *ACS Catal.* 7: 5316–5320.
93 Wang, Q., Cai, Z.-J., Liu, C.-X. et al. (2019). *J. Am. Chem. Soc.* 141: 9504–9510.
94 Kakiuchi, F., Le Gendre, P., Yamada, A. et al. (2000). *Tetrahedron Asymmetry* 11: 2647–2651.
95 Romero-Arenas, A., Hornillos, V., Iglesias-Sigüenza, J. et al. (2020). *J. Am. Chem. Soc.* 142: 2628–2639.
96 Guo, Y., Liu, M.-M., Zhu, X. et al. (2021). *Angew. Chem. Int. Ed.* 60: 13887–13891.
97 López, L.A. and López, E. (2015). *Dalton Trans.* 44: 10128–10135.
98 Gao, D.-W., Gu, Q., Zheng, C. et al. (2017). *Acc. Chem. Res.* 50: 351–365.
99 Liu, C.X., Gu, Q., and You, S.-L. (2020). *Trends Chem.* 2: 737–749.
100 Pi, C., Li, Y., Cui, X. et al. (2013). *Chem. Sci.* 4: 2675–2679.
101 Gao, D.W., Shi, Y.C., Gu, Q. et al. (2013). *J. Am. Chem. Soc.* 135: 86–89.
102 Shi, Y.C., Yang, R.F., Gao, D.W. et al. (2013). *Beilstein J. Org. Chem.* 9: 1891–1896.
103 Gao, D.-W., Gu, Q., and You, S.-L. (2016). *J. Am. Chem. Soc.* 138: 2544–2547.
104 Cai, Z.-J., Liu, C.-X., Gu, Q. et al. (2019). *Angew. Chem. Int. Ed.* 58: 2149–2153.

105 Pi, C., Cui, X., Liu, X. et al. (2014). *Org. Lett.* 16: 5164–5167.
106 Huang, Y., Pi, C., Cui, X. et al. (2020). *Adv. Synth. Catal.* 362: 1385–1390.
107 Xu, J., Liu, Y., Zhang, J. et al. (2018). *Chem. Commun.* 54: 689–692.
108 Lou, S.-J., Zhuo, Q., Nishiura, M. et al. (2021). *J. Am. Chem. Soc.* 143: 2470–2476.
109 Liu, Y.-H., Li, P.-X., Yao, Q.-J. et al. (2019). *Org. Lett.* 21: 1895–1899.
110 Liu, L., Song, H., Liu, Y.-H. et al. (2020). *ACS Catal.* 10: 7117–7122.
111 Batuecas, M., Luo, J., Gergelitsová, I. et al. (2019). *ACS Catal.* 9: 5268–5278.
112 Deng, R., Huang, Y., Ma, X. et al. (2014). *J. Am. Chem. Soc.* 136: 4472–4475.
113 Gao, D.-W., Yin, Q., Gu, Q. et al. (2014). *J. Am. Chem. Soc.* 136: 4841–4844.
114 Nottingham, C., Müller-Bunz, H., and Guiry, P.J. (2016). *Angew. Chem. Int. Ed.* 55: 11115–11119.
115 Gao, D.W., Zheng, C., Gu, Q. et al. (2015). *Organometallics* 34: 4618–4625.
116 Gao, D.-W., Gu, Y., Wang, S.-B. et al. (2016). *Organometallics* 35: 3227–3233.
117 Ma, X. and Gu, Z. (2014). *RSC Adv.* 4: 36241–36244.
118 Liu, L., Zhang, A.A., Zhao, R.J. et al. (2014). *Org. Lett.* 16: 5336–5338.
119 Xu, B.-B., Ye, J., Yuan, Y. et al. (2018). *ACS Catal.* 8: 11735–11740.
120 Cai, Z.-J., Liu, C.-X., Wang, Q. et al. (2019). *Nat. Commun.* 10: 4168.
121 Liu, C.-X., Cai, Z.-J., Wang, Q. et al. (2020). *CCS Chem.* 2: 642–651.
122 Luo, S., Xiong, Z., Lu, Y. et al. (2018). *Org. Lett.* 20: 1837–1840.
123 Jia, L., Liu, X., Zhang, A.A. et al. (2020). *Chem. Commun.* 56: 1737–1740.
124 Shibata, T. and Shizuno, T. (2014). *Angew. Chem. Int. Ed.* 53: 5410–5413.
125 Zhang, Q.-W., An, K., Liu, L.-C. et al. (2015). *Angew. Chem. Int. Ed.* 54: 6918–6921.
126 Murai, M., Matsumoto, K., Takeuchi, Y. et al. (2015). *Org. Lett.* 17: 3102–3105.
127 Shibata, T., Shizuno, T., and Sasaki, T. (2015). *Chem. Commun.* 51: 7802–7804.
128 Zhao, W.T., Lu, Z.Q., Zheng, H. et al. (2018). *ACS Catal.* 8: 7997–8005.
129 Chen, H., Wang, Y.-X., Luan, Y.-X. et al. (2020). *Angew. Chem. Int. Ed.* 59: 9428–9432.